FULL WAVE SYNTHETIC ACOUSTIC LOGS IN SATURATED POROUS MEDIA PART I: A REVIEW OF BIOT'S THEORY

by

D.P. Schmitt

Earth Resources Laboratory
Department of Earth, Atmospheric, and Planetary Sciences
Massachusetts Institute of Technology
Cambridge, MA 02139

Abstract

Hydrocarbon exploration is especially concerned with two phase media. Following Biot, such finite porosity rocks are modeled as statistically isotropic materials composed of a solid elastic matrix permeated by a network of interconnected pores saturated with a compressible viscous liquid.
In a first step, the constitutive equations of a saturated porous medium are reviewed, using mixtures theory and homogenization theory. This study focuses on the assumptions which are necessary but not always explicit. Biot's formulation is then modified by the introduction of a unified definition of the viscous and mass coupling coefficients which are both frequency dependent. The continuity equations at different kinds of interfaces are also analyzed.
The body wave velocities and attenuations are then computed, using the cylindrical duct model for pores. The effects of the saturant fluid, the permeability and the porosity are studied.

INTRODUCTION

Beyond the study of the macroscopic dynamic behavior of a fully saturated porous medium, Biot's theory (1956a, b; 1962) allows the analysis of the propagation of a total wavefield as for the solid elastic media. The porous formation is modelled by a statistically isotropic two phase medium composed of a solid elastic matrix permeated by a network of interconnected pores saturated by a compressible viscous liquid. The seismic wavelength is assumed to be large compared to the characteristic pore dimension (i.e., no diffraction). Although this model has been the basis for numerous theoretical studies, it was not until recently that Plona (1980) and Plona and Johnson (1980) experimentally demonstrated the validity of the theory. It predicts the existence of three types of body waves: a compressional wave of the first kind, which displays high velocity and quasi-elastic properties; a compressional wave of the second kind, associated with

low velocity and quasi-viscous characteristics; and a shear wave. All three body waves are dispersive and dissipative: their velocities are complex and frequency dependent.

Energy dissipation is due to the fluid flow related to the relative motion of the two phases which are coupled through friction and inertial forces. These forces are of the same order of magnitude for a so called "critical frequency" which depends on the saturant fluid characteristics, the porosity, and the permeability of the medium. Below this frequency, i.e., in the low frequency range, the viscous forces are predominant and the (laminar) flow follows Poiseuille's law. When the inertial forces are no longer negligible, a given repartition function of the stress in the fluid occurs (the flow is no longer uniform). In the high frequency range, the viscosity effects take place in only a very thin layer close to the pore wall. The dissipation of energy, in the sense of the inverse of the quality factor, is maximum around the critical frequency.

One has to keep in mind that Biot's model is a model which accounts for *only one attenuation mechanism.* It should not be applied universally. It is only a tool, among several others, for the interpretation in terms of lithology and petrophysics of the information produced by the P and S waves.

The description of the dynamic behavior of a saturated porous medium is essentially phenomenological in the sense that the exact motion of the fluid is not described. Biot's formulations (1956a, b; 1962) are based on the Hamilton principle, the Lagrangian description of the medium in the frame of continuum mechanics. As pointed out by Coussy and Bourbié (1984) and Bonnet (1985), the approaches are *a priori* phenomenological and heuristic. The problem consists in the formulation of the kinetic energy, the potential (deformation) energy and the dissipated energy. The two formulations of Biot (1956a, b; 1962) differ by the choice and the meaning of the generalized coordinates. The constitutive equations obtained are physically reasonable but the theoretical proof is not well established.

Homegenization theory (Auriault, 1980, 1981) allows a more rigorous approach. The basic assumption is that the medium is composed of spatially recurring fine (microscopic) structures. With constitutive equations for both components at the microscopic scale (the saturant fluid being Newtonian) as well as the pore geometry, the homogenization process leads to an exact expression of the constitutive equations at the macroscopic scale, provided that the pores are small (i.e., no diffraction). This technique is very mathematical. The resultant law of filtration corresponds to a generalized Darcy's law where a complex permeability function, which is frequency dependent and related to the pore shape, arises. The real and imaginary parts of this function can be physically interpreted in terms of dissipated viscous power and kinetic energy. Then, for a given pore geometry, the inertial and viscous coupling coefficients, required for the description of the dynamic behavior of a saturated porous medium, can be evaluated (Avallet, 1981; Borne, 1983; Auriault et al., 1985).

In this review, Bonnet's (1985) and Schmitt's (1985) formulation which uses the

mixtures theory (Truesdell and Toupin, 1960) is followed. The constituents are separated and the macroscopic constitutive equations, related to the irreversible process, are deduced from the analysis of the forces exerted by one another. The constitutive equations obtained include a frequency dependence of the mass coupling coefficient, in accordance with the homogenization theory. The continuity equations at the different kinds of interfaces are also reviewed.

With the pores modelled as cylindrical ducts with an unidirectional flow, the properties of the body wave velocities and attenuations as a function of the saturant fluid, the permeability and the porosity are then studied.

NOTATIONS

The phenomenological variables are defined at the macroscopic scale.

- $\tilde{\phi}$: porosity of the material.
- $\tilde{k}$: intrinsic permeability of the porous medium.
- η: dynamic viscosity of the saturant fluid.
- ρ_s: density of the constitutive grains (i.e., the solid).
- ρ_f: density of the saturant fluid.
- $\rho_1 = (1 - \tilde{\phi})\rho_s$: solid phase density per unit volume of the porous medium.
- $\rho_2 = \tilde{\phi}\rho_f$: liquid phase density per unit volume of the porous medium.

The total density of the porous material is:

$$\rho = \rho_1 + \rho_2 \tag{1}$$

- $\vec{u} = (u_1, u_2, u_3)^T$: mean displacement vector of the solid
- $\vec{U} = (U_1, U_2, U_3)^T$: mean displacement vector of the fluid.

These displacements are defined so that the products $\rho_1 u_i$ and $\rho_2 U_i$ by a surface element dS represent the mass flux through this surface.
The internal force of each constituent is characterized by a stress tensor:

- $\underline{\sigma}$ for the solid (σ_{ij})
- $\underline{\mathbf{S}}$ for the fluid (S_{ij})
- $e_{ij} = \frac{1}{2}(\partial_i u_j + \partial_j u_i)$ is the strain in the solid (elements of a tensor $\underline{\mathbf{E}}$).
- $\varepsilon_{ij} = \frac{1}{2}(\partial_i U_j + \partial_j U_i)$ is the strain in the fluid.

Einstein's convention is used so that the respective dilatation for the solid and the fluid are:

$$e = e_{ii} = \partial_i u_i \tag{2}$$
$$\varepsilon = \epsilon_{ii} = \partial_i U_i \tag{3}$$

The dot convention is also used, i.e. : $dx/dt = \dot{x}$ and $dx^2/dt^2 = \ddot{x}$

- δ_{ij} is the Kronecker delta (i.e., the unit tensor)

ASSUMPTIONS

1. The porous medium is saturated and statistically isotropic.
2. The matrix is elastic and isotropic.
3. The saturant fluid is a Newtonian viscous liquid.
4. The liquid phase is continuous. The occluded pores are then implicitly included in the matrix.
5. The study is made in the frame of the linear theory of elasticity (i.e., small perturbations).
6. The process is purely mechanical (no thermomechanical coupling, for example , is considered).
7. The physical system is at equilibrium when at rest.
8. The wavelength is supposed to be large compared to the characteristic pore dimension (i.e., no diffraction).
9. The stress, as well as the densities, of the solid and the liquid are of the same order of magnitude.

The above are the usual assumptions. In addition,

10. As for a viscous Newtonian liquid, the stress tensor of the saturant fluid can be separated in an elastic part and in a viscous part. Thus,

$$S_{ij} = s\delta_{ij} + \Sigma_{ij} \tag{4}$$

where

- s depends only on the state variables u_i, $U_i\,(e,\,\varepsilon)$. This is the "partial" tension of the saturant fluid, related to the pressure p in the pores by:

$$s = -\tilde{\phi}p \tag{5}$$

- Σ_{ij} only depends on the velocities $\dot{u}_i$, $\dot{U}_i\,(\dot{e},\,\dot{\varepsilon})$. This is the viscous stress.

11. The constitutive equation of the saturant fluid is analogous to the one of a Newtonian fluid. Then, the viscous stress is given by:

$$\Sigma_{ij} = \lambda_0\tilde{\phi}\varepsilon_{ii}\delta_{ij} + 2\mu_0\tilde{\phi}\varepsilon_{ij} \tag{6}$$

where λ_0 and μ_0 are the viscous constants of the fluid.

DYNAMICS EQUATIONS

Balance of momentum

The balance of momentum is evaluated through the Lagrange equations because mixtures theory does not allow a formulation which could be easily explained physically (Bonnet, 1985). The generalized coordinates are the displacement coordinates u_i and U_i as in Biot (1956a).

Denoting T the kinetic energy of the system per unit volume, the equations are (for the i-th coordinate):

$$\begin{cases} \frac{\partial}{\partial t}(\frac{\partial T}{\partial \dot{u}_i}) &= \partial \sigma_{ij} + \rho_1 f_{1i} - \lambda_{1i} \\ \frac{\partial}{\partial t}(\frac{\partial T}{\partial \dot{U}_i}) &= \partial_j S_{ij} + \rho_2 f_{2i} - \lambda_{2i} \end{cases} \tag{7}$$

where

- $\frac{\partial}{\partial t}(\frac{\partial T}{\partial \dot{x}_i})$ represents the "acceleration" of a constituent per unit volume ($\dot{x}_i = \dot{u}_i$ for the solid; $\dot{x}_i = \dot{U}_i$ for the fluid).
- f_{1i} (f_{2i}) is the force per unit mass exerted at distance on the solid (the fluid).
- $-\lambda_{1i}$ ($-\lambda_{2i}$) is the force exerted per unit volume on the solid (the fluid) by the fluid (the solid). Following mixtures theory it is called the "source of momentum".

In a reference system related to the solid, and for a motion in the i direction, the kinetic energy can be written (α denoting the inhomogeneity of the velocities):

$$T_{s(i)} = \frac{1}{2}\rho_2 \bar{V}_2^2 = \frac{1}{2}\rho_2 \alpha (\dot{U}_i - \dot{u}_i)^2 \tag{8}$$

where $\bar{V}_2^2$ represents the mean quadratic velocity of the fluid:

$$\bar{V}_2 = \sqrt{\alpha}\,(\dot{U}_i - \dot{u}_i) \quad \text{with } \alpha > 1$$

The local field velocity and α term depend on the angular frequency ω.

In a fixed reference, the kinetic energy, in the i direction, is then:

$$T_{(i)} = \frac{1}{2}\dot{U}_i^2 \rho_2 \alpha + \dot{u}_i \dot{U}_i \rho_2 (1-\alpha) + \frac{1}{2}\dot{u}_i^2 (\rho_2 \alpha + \rho_1 - \rho_2) \tag{9}$$

Because of the isotropy of the material, for a motion in any direction, the kinetic energy may be written in a fixed reference:

$$2T = \alpha_{11} \sum_{i=1}^{3} \dot{u}_i^2 + 2\alpha_{12} \sum_{i=1}^{3} \dot{u}_i \dot{U}_i + \alpha_{22} \sum_{i=1}^{3} \dot{U}_i^2 \tag{10}$$

where

$$\begin{cases} \alpha_{11} &= \rho_1 + \rho_2(\alpha - 1) \\ \alpha_{12} &= \rho_2(1 - \alpha) \\ \alpha_{22} &= \rho_2 \alpha \end{cases}$$

The α_{ij} parameters, which are frequency dependent through α, characterize the inhomogeneity of the velocities and the notion of apparent volumetric mass.

When the fluid is at rest ($\dot{u}_i = \dot{U}_i$), the kinetic energy is simply:

$$2T = (\rho_1 + \rho_2) \sum_{i=1}^{3} \dot{u}_i{}^2 = \rho \sum_{i=1}^{3} \dot{u}_i{}^2$$

Introducing the expression (10) in the equations (7), the dynamic's law in its most general form is obtained:

$$\begin{cases} \partial_j \sigma_{ij} &= \alpha_{11} \ddot{u}_i + \alpha_{12} \ddot{U}_i - \rho_1 f_{1i} + \lambda_{1i} \\ \partial_j S_{ij} &= \alpha_{12} \ddot{u}_i + \alpha_{22} \ddot{U}_i - \rho_2 f_{2i} + \lambda_{2i} \end{cases} \tag{11}$$

Subsequently, the forces at distance (i.e., $f_{1i} = f_{2i} = 0$) are not taken into account. The reference equations are then:

$$\begin{cases} \partial_j \sigma_{ij} &= \alpha_{11} \ddot{u}_i + \alpha_{12} \ddot{U}_i + \lambda_{1i} \\ \partial_j S_{ij} &= \alpha_{12} \ddot{u}_i + \alpha_{22} \ddot{U}_i + \lambda_{2i} \end{cases} \tag{12}$$

Stress-strain relations

Biot's presentation (1956a) is here followed. In the frame of the linear theory of elasticity, the stresses (σ_{ij} and $s\delta_{ij}$) are linearly related to the strains (e_{ij} and ε). The porous medium being statistically isotropic, the directions of the principal stress and principal strains coincide. As for the isotropic elastic media, one then can write in these directions:

$$\begin{cases} \sigma_{IJ} &= 2N e_{IJ} + (Ae + Q\varepsilon)\delta_{IJ} \\ s\delta_{IJ} &= (\tilde{Q}e + \tilde{R}\varepsilon)\delta_{IJ} \end{cases} \tag{13}$$

In the absence of dissipation, the system is conservative and stable. The strains are small perturbations with respect to a minimum potential energy state. The total

differential of this energy W is:

$$dW = \frac{\partial W}{\partial e_{ij}} de_{ij} + \frac{\partial W}{\partial \varepsilon} d\varepsilon \tag{14}$$

where

$$\frac{\partial W}{\partial e_{ij}} = \sigma_{ij} \ , \ \frac{\partial W}{\partial \varepsilon} = s$$

W is a positive definite quadratic form which can be expressed, especially, in terms of the invariants of the strain tensor $\underline{\mathbf{E}}$. One then can rewrite equations (13) for any orientation of the coordinates axes. In addition, because of the tensor's invariants, the matrix of the system has to be symmetric so that $\tilde{Q} = Q$. Then:

$$\begin{cases} \sigma_{ij} &= 2Ne_{ij} + (Ae + Q\varepsilon)\delta_{ij} \\ s\delta_{ij} &= (Qe + \tilde{R}\varepsilon)\delta_{ij} \end{cases} \tag{15}$$

A and N are then equivalent to Lamé's coefficients. $\tilde{R}$ is a measure of the fluid pressure needed to move a given fluid volume into the porous aggregate, the total volume being constant. Q is related to the fluid and solid volume variations.

Following Biot and Willis (1957) and Chandler and Johnson (1981), Bonnet (1985) presents experiments which allow interpretation of the physical meaning of these parameters. They can be easily expressed as functions of the bulk modulii of the solid K_s, the skeleton K_b and the fluid K_f, the shear modulus of the skeleton μ_b and the porosity $\tilde{\phi}$. Following Plona and Johnson (1980), one has:

$$\begin{cases} A &= \dfrac{(1-\tilde{\phi})(1-\tilde{\phi}-\dfrac{K_b}{K_s})K_s + \tilde{\phi}\dfrac{K_s}{K_f}K_b}{1-\tilde{\phi}-\dfrac{K_b}{K_s}+\tilde{\phi}\dfrac{K_s}{K_f}} - \dfrac{2}{3} \\ Q &= \dfrac{(1-\tilde{\phi}-\dfrac{K_b}{K_s})\tilde{\phi}K_s}{1-\tilde{\phi}-\dfrac{K_b}{K_s}+\tilde{\phi}\dfrac{K_s}{K_f}} \\ \tilde{R} &= \dfrac{\tilde{\phi}^2 K_s}{1-\tilde{\phi}-\dfrac{K_b}{K_s}+\tilde{\phi}\dfrac{K_s}{K_f}} \\ N &= \mu_b \end{cases} \tag{16}$$

Denoting α_m and β_m, the compressional and shear wave velocities of the dry rock, one can write:

$$\begin{aligned} K_b &= (1-\tilde{\phi})\rho_s(\alpha_m^2 - 4\beta_m^2/3) \\ N &= (1-\tilde{\phi})\rho_s\beta_m^2 \end{aligned} \tag{17}$$

while for the fluid

$$K_f = \rho_f \alpha_m^2$$

If one assumes an anelastic attenuation for the P and S waves in the skeleton characterized by quality factors Q_{α_m} and Q_{β_m} and a frequency dependence $e^{i\omega t}$, it implies a velocity dispersion of the form, (e.g. Aki and Richards, 1980):

$$c(\omega) = \frac{c(\omega_0)}{\left(1 - \frac{1}{\pi Q}\mathrm{Log}(\frac{\omega}{\omega_0})\right)(1 - \frac{i}{2Q})} \tag{18}$$

where

- ω_0 is a reference angular frequency
- c(ω) is the body wave velocity (α_m or β_m) at angular frequency ω,
- Q is the corresponding quality factor (Q_{α_m} or Q_{β_m}).

In these conditions, α_m and β_m become complex and frequency dependent as well as K_b and the coefficients A, N, Q and $\tilde{R}$.

Expression of the source of momentum

The complete resolution of the equations (12) needs the expression of the force per unit volume exerted by the fluid (the solid) on the solid (the fluid), i.e. $-\lambda_{1i}$ $(-\lambda_{2i})$.

Assuming that the porous medium is granular, the force exerted by the fluid on an assumed spherical grain is studied. Classical hydrodynamics (Landau and Lifschitz, 1971) states that the force exerted on a sphere with harmonic motion in a Newtonian fluid is given by:

$$\vec{f} = -a(\omega)\vec{v} - m_a(\omega)\vec{\gamma} \tag{19}$$

where

- $\vec{v}$ and $\vec{\gamma}$ are, respectively, the sphere velocity and acceleration,
- ω is the angular frequency,
- a is a coefficient proportional to the viscosity at low frequencies,

- m_a is the "associated mass".

a and m_a are constant at low frequencies.

The existence of these two types of forces may then be predicted in the case of a porous medium. The viscous forces are related to the velocity while the inertial (coupling) forces are related to the acceleration. The force exerted per unit volume on the solid skeleton may be written:

$$-\lambda_{1i} = -b(\dot{u}_i - \dot{U}_i) \tag{20}$$

The inertial coupling, related to the notion of apparent volumetric mass, is already taken into account (implicitly) in the kinetic energy formulation (eq. 10) through the α_{ij} parameters which are frequency dependent.

Darcy's law (quasi-static) given by:

$$\vec{V} = -\frac{\tilde{k}}{\eta}\nabla p \tag{21}$$

where

- $\vec{V}$ is the filtration velocity of the fluid
- p is the pore pressure,

must be verified at low frequencies so that :

$$\lim_{\omega \to 0} b = \frac{\eta \tilde{\phi}^2}{\tilde{k}} \tag{22}$$

Dynamic equations

Putting equations (20) and (4) into the system (12) one obtains:

$$\begin{cases} \partial_j \sigma_{ij} & = & \rho_{11}\ddot{u}_i + \rho_{12}\ddot{U}_i + b(\dot{u}_i - \dot{U}_i) \\ \partial_j(s\delta_{ij} + \Sigma_{ij}) & = & \rho_{12}\ddot{u}_i + \rho_{22}\ddot{U}_i - b(\dot{u}_i - \dot{U}_i) \end{cases} \tag{23}$$

where

$$\begin{cases} \rho_{11} = \alpha_{11} = \rho_1 - \rho_2(1-\alpha) \\ \rho_{12} = \alpha_{12} = \rho_2(1-\alpha) \\ \rho_{22} = \alpha_{22} = \rho_2\alpha \end{cases}$$

Using equations (6) and (15), Bonnet (1985) demonstrated that the terms related to the fluid viscosity can be considered as negligible with respect to the elastic terms. An additional **assumption** is then:

12. *The viscous stress of the saturant fluid is negligible with respect to its tension.*

The equations (23) may thus be written:

$$\begin{cases} \partial_j \sigma_{ij} &= \rho_{11}\ddot{u}_i + \rho_{12}\ddot{U}_i + b(\dot{u}_i - \dot{U}_i) \\ \partial_i s &= \rho_{12}\ddot{u}_i + \rho_{22}\ddot{U}_i - b(\dot{u}_i - \dot{U}_i) \end{cases} \tag{24}$$

In this system of equations, the viscous coupling forces (related to b) and the inertial coupling forces (related to the parameters ρ_{ij}) are characterized. The equations are identical to those of Biot (1956a) because of the identical notations. The system (24), however, contains important differences:

- b is frequency dependent so that the variations of the stress repartition in the fluid are implicitly taken into account. It is unnecessary to distinguish the low and high frequency ranges to establish the equations.
- The coefficients ρ_{ij} are frequency dependent through only one function: $\alpha\rho_2$.
- The coefficients ρ_{ij} include two different physical phenomena through the parameters α_{ij}: the inhomogeneity of the velocities and the notion of apparent density.
- Last, assumption 12 was necessary.

Two situations are interesting:

a. *The fluid is at rest* : $\dot{U}_i = 0$
The second equation of the system (24) becomes, using equation (5),:

$$-\tilde{\phi}\partial_i p = \rho_{12}\ddot{u}_i - b\dot{u}_i \tag{25}$$

Therefore, a force, including an inertial and a viscous part, has to be exerted on the fluid so that it is at rest.

b. *No relative fluid-solid motion* : $\dot{u}_i = \dot{U}_i = \dot{d}_i$
The equation relative to s becomes (using equation (5)):

$$-\tilde{\phi}\partial_i p = (\rho_{12} + \rho_{22})\ddot{d}_i \tag{26}$$

The equation of motion of a perfect fluid whose density is ρ_f is:

$$-\partial_i p = \rho_f \ddot{d}_i \quad \text{i.e.} \quad -\tilde{\phi}\partial_i p = \tilde{\phi}\rho_f \ddot{d}_i \tag{27}$$

Equation (26) may be obtained using equation (21) with $b = 0$ (i.e., $\eta = 0$: perfect fluid), so that:

$$\tilde{\phi}\rho_f = \rho_2 = \rho_{12} + \rho_{22} \tag{28}$$

Using the expressions of the α_{ij} coefficients, the kinetic energy (equation (10)) becomes:

$$2T = (\rho_1 + \rho_2)\dot{d}_i\dot{d}i = (\rho_{11} + 2\rho_{12} + \rho_{22})\dot{d}_i\dot{d}_i \tag{29}$$

Therefore, using equation (28),:

$$\rho_1 = \rho_{11} + \rho_{12} \tag{30}$$

These are Biot's equations (1956a) relating the ρ_{ij} coefficients to the densities per unit volume of the porous medium (ρ_1 and ρ_2).

In a way, the similarity of the resulting dynamic equations with those of Biot (1956a), despite the physical meaning of some parameters, makes up an *a posteriori* proof of the introduction by this author of a "pseudo"-potential of dissipated energy given by:

$$D = b\,(\dot{u}_i - \dot{U}_i)(\dot{u}_i - \dot{U}_i)$$

which is a function of the relative motion between the two phases.

If the present demonstration is also axiomatic, it is, however, more physically based.

Discussion

In equation (24), with a classical frequency dependence of the form $e^{i\omega t}$, the "viscous" terms are proportional to ω while the inertial terms vary as ω^2. Therefore, at low frequencies, the latter terms are negligible. For example, Rice and Cleary (1981) demonstrated that at extremely low frequencies, for a plane radial flow in a homogeneous medium, the equations (24) are uncoupled. Therefore, it is interesting to characterize the porous medium by a characteristic frequency, f_c, which defines the high and low frequency ranges.

When the solid is motionless or "unconstrained", the equation (24) gives:

$$\begin{aligned} -\tilde{\phi}\partial_i p &= \rho_{22}\ddot{U}_i + b\dot{U}_i \\ \iff -\tilde{\phi}\partial_i p &= \left(-\rho_{22}\omega^2 + i\omega b\right) U_i \end{aligned} \tag{31}$$

The inertial terms will be negligible for:

$$\begin{aligned} \rho_{22}\omega^2 &\ll \omega b \\ \iff f &\ll f_{ci} = \frac{b}{2\pi\rho_{22}} \end{aligned} \tag{32}$$

Taking into account the "compatibility" relation (22) and considering that ρ_{22} and ρ_2 are of the same order of magnitude, one obtains the classical expression of the characteristic frequency:

$$f_c = \frac{\eta \tilde{\phi}^2}{2\pi \tilde{k} \rho_2} = \frac{\eta \tilde{\phi}}{2\pi \tilde{k} \rho_f} \tag{33}$$

In terms of flow, the definition is different. It brings in a characteristic pore dimension (a), perpendicular to the sense of the fluid motion, on account of the viscous drive phenomena. An acceleration of the rock produces tangential stresses in the fluid. These stresses decay exponentially away from the pore walls and are characterized by a "viscous skin depth" given by:

$$\delta = \sqrt{\frac{2\eta}{\omega \rho_f}} \tag{34}$$

It decreases when the frequency increases (unlike the stress). The flow will be uniform (Poiseuille's law) only at low frequencies when δ is much greater than the characteristic pore dimension (the viscous forces are predominant). If δ is of the order of magnitude of a, the flux is disturbed. The "critical" frequency is then:

$$\omega_c^* = \frac{2\eta}{a^2 \rho_f} \iff f_c^* = \frac{\eta}{\pi a^2 \rho_f} \tag{35}$$

This expression differs from Biot's equation (1956a). It corresponds to the frequency used by homogenization theory for a nondimensional formulation (Avallet, 1981; Borne, 1983; Auriault et al., 1985) and to the value given by Mavko and Nur (1979).

Intuitively, it is easy to predict that f_c^* is lower than f_c. In the case of cylindrical ducts, a simple proof can be given. Darcy's law, in its most well known formulation, may be written:

$$Q = \frac{\tilde{k}}{\eta} S \frac{P}{L} \tag{36}$$

where Q is the flow through a surface S of a medium of thickness L for a pressure difference P.

For cylindrical ducts of radius a, the classical form of Poiseuille's law is:

$$Q = \frac{\pi a^4}{8\eta} \frac{P}{L} \tag{37}$$

The compatibility of the last two equations leads to:

$$a^2 = 8 \frac{\tilde{k}}{\tilde{\phi}} \tag{38}$$

so that $f_c^* < f_c$.

In the following, because the formulation explicitly includes the frequency dependence of the coefficient b, and the energy dissipation related to the forces present is the interesting feature, the characteristic frequency will correspond to equation (33) while the critical frequency will correspond to equation (32).

Contribution of homogenization theory

Homogenization theory justifies the stress-strain relations (eq. 15) and assumption 12 through the equations of motion that come from it. Assumption 11 is not explicit but implicit (Auriault, 1980, 1981). In addition

- In the case of a motionless solid, the constitutive equation of the liquid at the macroscopic scale is:

$$\tilde{\phi}\dot{U}_i = -K(\omega)\nabla p \tag{39}$$

where p is the pore pressure.
K(ω) is a complex permeability function ("equivalent" to the hydraulic permeability $\tilde{k}/\eta$ because of Darcy's law) which may be computed for a given pore geometry by integration of the Navier-Stokes equations over a period. In the most general case, K(ω) is a symmetric complex tensor of order two, which is also positive and definite, and thus can be inverted.
If

$$H(\omega) = \frac{1}{K(\omega)} = H_1(\omega) + iH_2(\omega) \tag{40}$$

then $H_1(\omega)$ and $H_2(\omega)$ can be physically interpreted in terms of dissipated viscous power and kinetic energy (Avallet, 1981; Borne, 1983, Auriault et al., 1985).

- In the general case of a moving solid, the dynamic equations are identical to expressions (23) and (24). The coupling coefficients are then given by:

$$\begin{cases} \rho_{22}(\omega) &= \dfrac{\tilde{\phi}^2}{\omega} H_2(\omega) \\ \rho_{12}(\omega) &= \rho_2 - \rho_{22}(\omega) \\ \rho_{11}(\omega) &= \rho_1 - \rho_{12}(\omega) \\ b(\omega) &= \tilde{\phi}^2 H_1(\omega) \end{cases} \tag{41}$$

Beyond the frequency dependence and the relations between ρ_{ij} and the densities ρ_1, ρ_2 already established, equations (41) show that the viscous and mass coupling

coefficients are related to one another, contrary to what is usually stated, and are dependent on the pore shape.

From the practical point of view, ρ_{22}, which is assumed to be constant and frequency independent, is often related to a tortuosity factor θ. Plona and Johnson (1980) define:

$$\rho_{22} = \theta\tilde{\phi}\rho_f \quad \text{with} \quad \theta \geq 1 \tag{42}$$

and give the tortuosity, following Berryman (1980), as:

$$\theta = \frac{1}{2}\left(\frac{1}{\tilde{\phi}} + 1\right) \tag{43}$$

Brown (1980) uses the formation factor F obtained from the resistivity measurements:

$$R_f F = R_0 \tag{44}$$

where

- R_0 is the resistivity of the fully saturated permeable formation
- R_f is the fluid resistivity

As a matter of fact, these two definitions are very close to one another as the experiments showed that:

$$F = y\tilde{\phi}^{-m} \tag{45}$$

where

- m is a cementing factor (or tortuosity)
- y is a constant which depends on the lithology.

In addition, Sen et al. (1981) define ρ_{22} with equation (42) but with a θ equal to $\tilde{\phi}^{-x}$ ($x = \frac{1}{2}$ for identical spheres).

All these expressions come from high frequency measurements independent of $b(\omega)$ which is estimated through computation in the case of cylindrical pores. Bonnet (1985) carried out measurements of both $b(\omega)$ and $\rho_{22}(\omega)$ at low frequencies, up to the characteristic frequency, for a medium made of fused glass balls. If the results do not show any obvious differences with the high frequency measurements for ρ_{22} (only one pore geometry has been analyzed and the results are highly dependent on the precision of the measurements), the coefficient $b(\omega)$ does not correspond to the one of the cylindrical ducts. These results are confirmed by the measurements made by Borne (1983) (see also Auriault et al., 1985) in the whole frequency range for a synthetic porous medium where the pores are loop-holes.

WAVE EQUATIONS

Equations of motion

The equations of motion are obtained by putting the system (15) into the equations (24). The porous medium being statistically isotropic, $\partial_i N = \partial_i Q = \partial_i \tilde{R} = \partial_i A = 0$. One then obtains:

$$\left\{ \begin{array}{rcl} N(\partial_j\partial_i u_j + \partial_j\partial_j u_i) + A\partial_i\partial_k u_k + Q\partial_i\partial_k U_k &=& \rho_{11}\ddot{u}_i + \rho_{12}\ddot{U}_i + b(\dot{u}_i - \dot{U}_i) \\ Q\partial_i\partial_k u_k + \tilde{R}\partial_i\partial_k U_k &=& \rho_{12}\ddot{u}_i + \rho_{22}\ddot{U}_i - b(\dot{u}_i - \dot{U}_i) \end{array} \right. \tag{46}$$

or

$$\left\{ \begin{array}{rcl} (A+N)\mathrm{graddiv}\vec{u} + N\nabla^2\vec{u} + Q\mathrm{graddiv}\vec{U} &=& \rho_{11}\ddot{\vec{u}} + \rho_{12}\ddot{\vec{U}} + b(\dot{\vec{u}} - \dot{\vec{U}}) \\ Q\mathrm{graddiv}\vec{u} + \tilde{R}\mathrm{graddiv}\vec{U} &=& \rho_{12}\ddot{\vec{u}} + \rho_{22}\ddot{\vec{U}} - b(\dot{\vec{u}} - \dot{\vec{U}}) \end{array} \right. \tag{47}$$

where ∇^2 is the Laplacian operator.
The divergence of the system (46) is:

$$\left\{ \begin{array}{rcl} (A+N)\partial_i\partial_i\partial_k u_k + N\partial_i\partial_j\partial_j u_i + Q\partial_i\partial_i\partial_k U_k & & \\ = \rho_{11}\dfrac{\partial^2}{\partial t^2}(\partial_i u_i) + \rho_{12}\dfrac{\partial^2}{\partial t^2}(\partial_i U_i) + b\dfrac{\partial}{\partial t}(\partial_i u_i - \partial_i U_i) & & \\ Q\partial_i\partial_i\partial_k u_k + \tilde{R}\partial_i\partial_i\partial_k U_k & & \\ = \rho_{12}\dfrac{\partial^2}{\partial t^2}(\partial_i u_i) + \rho_{22}\dfrac{\partial^2}{\partial t^2}(\partial_i U_i) - b\dfrac{\partial}{\partial t}(\partial_i u_i - \partial_i U_i) & & \end{array} \right.$$

or

$$\left\{ \begin{array}{rcl} P\nabla^2 e + Q\nabla^2\varepsilon &=& \rho_{11}\ddot{e} + \rho_{12}\ddot{\varepsilon} + b(\dot{e} - \dot{\varepsilon}) \\ Q\nabla^2 e + \tilde{R}\nabla^2\varepsilon &=& \rho_{12}\ddot{e} + \rho_{22}\ddot{\varepsilon} - b(\dot{e} - \dot{\varepsilon}) \end{array} \right. \tag{48}$$

where $P = A + 2N$.

Taking the curl of the equations (46) written for the j-th coordinate, one obtains:

$$\left\{ \begin{array}{rcl} & & (A+N)\varepsilon_{ijk}\partial_i\partial_j\partial_l u_l + N\varepsilon_{ijk}\partial_i\partial_j\partial_l u_j + Q\varepsilon_{ijk}\partial_i\partial_j\partial_l U_l \\ &=& \rho_{11}\dfrac{\partial^2}{\partial t^2}(\varepsilon_{ijk}\partial_i u_j) + \rho_{12}\dfrac{\partial^2}{\partial t^2}(\varepsilon_{ijk}\partial_i U_i) + b\dfrac{\partial}{\partial t}\varepsilon_{ijk}(\partial_i u_j - \partial_i U_j) \\ & & Q\varepsilon_{ijk}\partial_i\partial_j\partial_l u_l + \tilde{R}\varepsilon_{ijk}\partial i\partial_j\partial_l Ul \\ &=& \rho_{12}\dfrac{\partial^2}{\partial t^2}(\varepsilon_{ijk}\partial_i u_j) + \rho_{22}\dfrac{\partial^2}{\partial t^2}(\varepsilon_{ijk}\partial_i U_j) - b\dfrac{\partial}{\partial t}\varepsilon_{ijk}(\partial_i u_j - \partial_i U_j) \end{array} \right.$$

or

$$\left\{ \begin{array}{rcl} N\nabla^2\mathrm{curl}\vec{u} &=& \rho 11\dfrac{\partial^2}{\partial t^2}(\mathrm{curl}\vec{u}) + \rho_{12}\dfrac{\partial^2}{\partial t^2}(\mathrm{curl}\vec{U}) + b\dfrac{\partial}{\partial t}(\mathrm{curl}\vec{u} - \mathrm{curl}\vec{U}) \\ 0 &=& \rho_{12}\dfrac{\partial^2}{\partial t^2}(\mathrm{curl}\vec{u}) + \rho_{22}\dfrac{\partial^2}{\partial t^2}(\mathrm{curl}\vec{U}) - b\dfrac{\partial}{\partial t}(\mathrm{curl}\vec{u} - \mathrm{curl}\vec{U}) \end{array} \right. \tag{49}$$

The systems (48) and (49) bring in only dilatations and rotations. The compressional and shear waves of the porous medium are then uncoupled, just as for the isotropic elastic media.

Wave propagation

In order to solve the wave equation, as in the elastic case, the scalar (Φ) and vector ($\vec{\Psi}$) displacement potentials are introduced. They are defined by:

$$\begin{cases} \vec{u} &= (\mathrm{grad}\Phi^{(s)} + \mathrm{curl}\vec{\Psi}^{(s)})e^{i\omega t} \\ \vec{U} &= (\mathrm{grad}\Phi^{(l)} + \mathrm{curl}\vec{\Psi}^{(l)})e^{i\omega t} \end{cases} \tag{50}$$

with $\mathrm{div}\vec{\Psi}^{(s)} = \mathrm{div}\vec{\Psi}^{(l)} = 0$.

Compressional waves

Using equations (50), the divergence of equations (46) may be written:

$$\begin{cases} P\nabla^2\Phi^{(s)} + Q\nabla^2\Phi^{(l)} &= -\omega^2(\gamma_{11}\Phi^{(s)} + \gamma_{12}\Phi^{(l)}) \\ Q\nabla^2\Phi^{(s)} + \tilde{R}\nabla^2\Phi^{(l)} &= -\omega^2(\gamma_{12}\Phi^{(s)} + \gamma_{22}\Phi^{(l)}) \end{cases} \tag{51}$$

where

$$\gamma_{ii} = \rho_{ii}(\omega) - ib(\omega)/\omega \quad \gamma_{12} = \rho_{12}(\omega) + ib(\omega)/\omega$$

After some algebraic manipulations, one obtains from the last equations:

$$\Phi^{(l)} = \frac{1}{\omega^2}\frac{P\tilde{R} - Q^2}{Q\gamma_{22} - \tilde{R}\gamma_{12}}\nabla^2\Phi^{(s)} + \frac{\tilde{R}\gamma_{11} - Q\gamma_{12}}{Q\gamma_{22} - \tilde{R}\gamma_{12}}\Phi^{(s)} \tag{52}$$

so that $\Phi^{(s)}$ is the solution of:

$$(P\tilde{R} - Q^2)\nabla^4\Phi^{(s)} + \omega^2(P\gamma_{22} + \tilde{R}\gamma_{11} - 2Q\gamma_{12})\nabla^2\Phi^{(s)} + \omega^4(\gamma_{11}\gamma_{22} - \gamma_{12}^2)\Phi^{(s)} = 0 \tag{53}$$

$\Phi^{(s)}$ may then be expressed as the sum of two potentials, i.e. $\Phi^{(s)} = \Phi_1 + \Phi_2$, which satisfy Helmoltz type equations:

$$\nabla^2\Phi_j = -\frac{\omega^2}{\alpha_j^2}\Phi_j \quad j = 1,2 \tag{54}$$

for which the velocities α_j are solutions of the bi-quadratic equation deduced from relation (53):

$$\alpha^4(\gamma_{22}\gamma_{11} - \gamma_{12}^2) - \alpha^2(P\gamma_{22} + \tilde{R}\gamma_{11} - 2Q\gamma_{12}) + P\tilde{R} - Q^2 = 0 \tag{55}$$

Because the γ_{ij} terms are complex and frequency dependent, the velocities α_1 and α_2 are also complex and frequency dependent. The associated waves are then dispersive and

dissipative. P_1 will denote the wave corresponding to the greater velocity α_1 (analogous to the P wave of a single phase medium), and P_2 the other wave, usually called the slow P wave.

The scalar potential $\Phi^{(l)}$ relative to the saturant fluid is then:

$$\Phi^{(l)} = \sum_{j=1}^{2} \xi_j \Phi_j \tag{56}$$

where

$$\xi_j = -\frac{1}{\alpha_j^2} \frac{P\tilde{R} - Q^2}{Q\gamma_{22} - \tilde{R}\gamma_{12}} + \frac{\tilde{R}\gamma_{11} - Q\gamma_{12}}{Q\gamma_{22} - \tilde{R}\gamma_{12}}$$

The P_1 and P_2 waves *are not* respectively related to the solid and to the fluid. They correspond to singular motions of the fluid-solid system. In the absence of dissipation (i.e. $b = 0$ case) the velocities are real. Biot (1956a) demonstrated that:

- The P_1 wave corresponds to an in phase motion of the fluid and the solid,
- The P_2 wave corresponds to an out of phase motion of the fluid and the solid.

Plona and Johnson (1980) experimentally demonstrated the existence of the slow P wave using artificial porous materials. Their results, especially from the point of view of the velocity, agree well with theory (see Dutta, 1980; Berryman, 1980).

Shear wave

Using equations (50), the curl of equations (46) may be expressed as:

$$\begin{cases} N\nabla^2\vec{\Psi}^{(s)} &= -\omega^2(\gamma_{11}\vec{\Psi}^{(s)} + \gamma_{12}\vec{\Psi}^{(l)}) \\ \vec{\Psi}^{(l)} &= -\dfrac{\gamma_{12}}{\gamma_{22}}\vec{\Psi}^{(s)} = \chi\vec{\Psi}^{(s)} \end{cases} \tag{57}$$

so that the S wave velocity of the porous material is:

$$\beta = (N/(\gamma_{11} - \frac{\gamma_{12}^2}{\gamma_{22}}))^{\frac{1}{2}} \tag{58}$$

The fluid does not support any shear displacement. It affects the S wave, however, through inertial effects.

Summary

The system (50) may be finally written:

$$\left\{ \begin{array}{rcl} \vec{u} & = & \left\{ \sum_{j=1}^{2} \mathrm{grad}\Phi_j + \mathrm{curl}\vec{\Psi} \right\} e^{i\omega t} \\ \vec{U} & = & \left\{ \sum_{j=1}^{2} \xi_j \mathrm{grad}\Phi_j + \chi \mathrm{curl}\vec{\Psi} \right\} e^{i\omega t} \end{array} \right. \tag{59}$$

where the potentials Φ_j and $\vec{\Psi}$ satisfy Helmoltz type equations relative to the three complex body wave velocities (see equations (55) and (58)). ξ_j and χ are complex frequency dependent factors which characterize the influence of one phase on the other one due to dynamic and viscous forces.

CONTINUITY EQUATIONS

Few authors discuss the conditions at the interface between two porous media. Using the working rate of the forces acting on a saturated porous medium, Deresiewick and Skalak (1963) established sufficient conditions which ensure the uniqueness of the wave-field. They obtained a theorem similar to the one of Neumann for the elastic media. Rosenbaum (1974) and Feng and Johnson (1983a, b) applied these conditions to the case of a fluid-saturated porous medium interface.

Bonnet (1985) stated the continuity equations at the interface betweeen two porous media saturated by the same fluid. He separated the equations that can be inferred from the general principles of mechanics (using mixtures theory, porous media can be considered as a continuum) from the others. Here, this formulation is followed and extended to different situations.

Let $\vec{n}$, whose components are n_j, be the normal of the interface between two media indicated by the superscripts (1) and (2). Subsequently, the indices n and s will denote the normal and tangential components of the displacements or the stress. For simplicity, $[X^{(j)}]$ will denote $X^{(1)} - X^{(2)}$.

Porous-porous interface. Saturation by the same fluid

General principles of mechanics

Balance of mass The balance of mass along a surface of discontinuity in the bosom of a medium, which is a continuum in other respects, may be written (Truesdell and Toupin, 1960):

$$[\rho^{(j)}(v_i^{(j)} n_i - v_n^{(j)})] = 0 \tag{60}$$

where

- the superscript (j) denotes the parts on both sides of the discontinuity surface
- $\rho^{(j)}$ is the density of the medium,
- $v_i^{(j)}$ is the medium velocity,
- $v_n^{(j)}$ is the (normal) velocity of the discontinuity.

Using this expression in the case of two porous media considered as mixtures, one obtains (Truesdell and Toupin, 1960):

$$\left\{ \begin{array}{lcl} \rho^{(j)} & = & \rho_1^{(j)} + \rho_2^{(j)} \\ \rho^{(j)} v_i^{(j)} & = & \rho_1^{(j)} \dot{u}_i^{(j)} + \rho_2^{(j)} \dot{U}_i^{(j)} \end{array} \right. \tag{61}$$

$v_i^{(j)}$ is then the "inertial center" velocity.
Bonnet (1985) writes: "the discontinuity surface between two porous media moves with the velocity of the solid constituent" so that:

$$v_n^{(j)} = \dot{u}_i^{(j)} n_i \tag{62}$$

In fact, this means:

Assumption 13.

$$[\dot{u}_n^{(j)}] = 0 \tag{63}$$

This assumption is physically reasonable if the solid parts are supposed to keep in welded contact.

Using equations (61) and (62), the relation (60) may be written:

$$[\rho_2^{(j)}(\dot{U}_n^{(j)} - \dot{u}_n^{(j)})] \tag{64}$$

which becomes, with $\rho_2^{(j)} = \tilde{\phi}^{(j)}\rho_f$:

$$[\tilde{\phi}^{(j)}(\dot{U}_n^{(j)} - \dot{u}_n^{(j)})] = 0 \tag{65}$$

i.e. the flux is balanced.

Deresiewick and Skalak (1963) obtained the same relation (with the same assumption 13), but they do not say that this is only true for porous media saturated by equal density fluids.

Balance of momentum From Truesdell and Toupin (1960), the balance of momentum may be written:

$$[\Pi_{ik}^{(j)} n_k + \rho^{(j)} v_n^{(j)} v_i^{(j)}] = 0 \tag{66}$$

where $\Pi_{ik}^{(j)}$ is the stress tensor of the medium with:

$$\begin{aligned} \Pi_{ik}^{(j)} = \sigma_{ik}^{(j)} + S_{ik}^{(j)} \quad &- \quad \rho_1(\dot{u}_i^{(j)} - v_i^{(j)})(\dot{u}_k^{(j)} - v_k^{(j)}) \\ &- \quad \rho_2(\dot{U}_i^{(j)} - v_i^{(j)})(\dot{U}_k^{(j)} - v_k^{(j)}) \end{aligned} \tag{67}$$

Using equations (61) and (62), one gets:

$$\begin{aligned} [(\sigma_{ik}^{(j)} + S_{ik}^{(j)})n_k \quad &- \quad \rho_1(\dot{u}_i^{(j)} - v_i^{(j)})(\dot{u}_k^{(j)} - v_k^{(j)})n_k \\ &- \quad \rho_2(\dot{u}_i^{(j)} - v_i^{(j)})(\dot{U}_k^{(j)} - v_k^{(j)})n_k \\ &+ \quad (\rho_1 \dot{u}_i^{(j)} + \rho_2 \dot{U}_i^{(j)})\dot{u}_k^{(j)} n_k] = 0 \end{aligned} \tag{68}$$

14. *The terms which are a function of the constituent velocities are neglected with respect to their own stress.*

This assumption is also made by homogenization theory.

Then, the equation (68) reduces to the continuity of the sum of each constituent stress. Using assumptions 10 and 12:

$$[\sigma_{nn}^{(j)} + s^{(j)}] = 0 \tag{69}$$

$$[\sigma_{ns}^{(j)}] = 0 \tag{70}$$

Deresiewick and Skalak (1963) also obtained these equations but they pass over assumptions 1, 12 and 14 (this last one comes only from the present formulation).

Other relations

The solid parts have been already assumed to keep in welded contact. As for the solid elastic media, they are assumed to be well bonded so that the continuity of the solid displacements is ensured:

$$[u_n^{(j)}] = 0 \tag{71}$$

$$[u_s^{(j)}] = 0 \tag{72}$$

"Five" continuity equations have now been set up. The last one needed concerns the saturant fluid pressures:

$$[p^{(j)}] = 0 \tag{73}$$

Bonnet (1985) notices that there appears to be no effect of a pressure jump at the interface between two porous media within the dynamic state when the solid is motionless. When the solid cannot be distorted and within the steady state, the pressure jump is on the order of $\rho_f \alpha_f^2$ where α_f is the fluid velocity. Assuming that this relation is still valid for the dynamic motion of a deformable saturated porous medium, and taking into account the fourteenth assumption, the equation (73) is justified. It assumes, however, that the pores of both media are fully connected.

Without any theoretical demonstration, Deresiewick and Skalak (1963) state:

$$[p^{(j)}] = \varsigma \tilde{\phi}^{(j)} (\dot{U}_n^{(j)} - \dot{u}_n^{(j)}) \tag{74}$$

where ς is a resistance coefficient (or impedance, see Rosenbaum 1974).

The case for which the pores are fully connected corresponds to $\varsigma = 0$ (see Figure 1a). When the pores do not connect ς is infinite (see Figure 1c). There is no continuity

of the saturant fluid pressures and thus no relative motion (i.e. $\dot{U}_n^{(j)} = \dot{u}_n^{(j)} \quad j = 1, 2$) similar to the case of a solid-porous interface. A non zero finite value of ς should correspond to a partial communication of the pores (see Figure 1b) and thus a pressure jump. This intermediate situation is difficult to take into account: what is the value of ς ? How can it be practically determined ?

General porous-porous interface: Summary

When the porous media are saturated by two different fluids, only equations (65) and (73) need a demonstration. As a matter of fact, they are proved at the scale of the pores. Assuming that the interface between both fluids lies within a very short distance of the interface between the porous media, the same equations are obtained. The meaning is, however, different: there is no longer balance of the mass. Whatever the nature of the saturant fluid is, the combination of equations (63) and (65) leads to:

$$[\dot{u}_n^{(j)} + \tilde{\phi}^{(j)}(\dot{U}_n^{(j)} - \dot{u}_n^{(j)})] = 0 \tag{75}$$

which corresponds to balance of the fluid volume.

The general continuity equations may be written finally (with a temporal dependence of the form $e^{i\omega t}$):

$$\begin{cases} 1) & [u_n^{(j)}] = 0 \\ 2) & [u_s^{(j)}] = 0 \\ 3) & [\sigma_{nn}^{(j)} + s^{(j)}] = 0 \\ 4) & [\sigma_{ns}^{(j)}] = 0 \\ 5) & [p^{(j)}] = 0 \\ 6) & [\tilde{\phi}^{(j)}(U_n^{(j)} - u_n^{(j)})] = 0 \end{cases} \tag{76}$$

These are the classical continuity equations used at a porous-porous interface.

Elastic solid-porous interface

A solid elastic material can be considered as a zero porosity porous medium. Denoting by the superscript (2) the elastic medium, one obtains from the relations (76):

$$\begin{cases} 1) & u_n^{(1)} = u_n^{(2)} \\ 2) & u_s^{(1)} = u_s^{(2)} \\ 3) & \sigma_{nn}^{(1)} + s^{(1)} = \sigma_{nn}^{(2)} + s^{(2)} \\ 4) & \sigma_{ns}^{(1)} = \sigma_{ns}^{(2)} \\ 5) & U_n^{(1)} - u_n^{(1)} = 0 \end{cases} \tag{77}$$

Fluid-porous interface

In such a situation, two cases arise. The first one corresponds to a permeable interface (i.e., free fluid flow) while the second is relevant to the absence of relative motion between the two phases (i.e., impermeable interface). Contrary to what is stated by Rosenbaum (1974), this last case does not correspond, in the borehole configuration, to the presence of a mudcake. It is a limiting case for a zero thickness solid layer at the interface.

Permeable interface: free fluid flow

A fluid medium can be considered as a unit porosity porous medium. Therefore, following the same reasoning as for a porous-porous interface with $\tilde{\phi}^{(2)} = 1$ and $v_n^{(2)} = \dot{u}_n^{(1)}$, equation (64) becomes:

$$\tilde{\phi}^{(1)}(\dot{U}_n^{(1)} - \dot{u}_n^{(1)}) = \dot{U}_n^{(2)} - \dot{u}_n^{(1)} \tag{78}$$

This equation is still valid when the saturant fluid differs from the fluid medium, following the same reasoning as previously. Using a temporal dependence of the form $e^{i\omega t}$, the continuity equations may be written from (69), (70), (73) and (78):

$$\begin{cases} 1) & u_n^{(1)} + \tilde{\phi}^{(1)}(U_n^{(1)} - u_n^{(1)}) = U_n^{(2)} \\ 2) & \sigma_{nn}^{(1)} + s^{(1)} = \sigma_{nn}^{(2)} \\ 3) & \sigma_{ns}^{(1)} = 0 \\ 4) & p^{(1)} = p^{(2)} \end{cases} \tag{79}$$

Equation (3) comes from the fact that the fluid medium is assumed to be perfect.

Impermeable interface: occluded pores

The continuity equations can be easily inferred from the solid-porous relations (77). One simply needs to write the classical equations relative to a fluid-solid interface i.e. :

$$u_n^{(2)} = U_n^{(3)}; \quad \sigma_{nn}^{(2)} = \sigma_{nn}^{(3)}; \quad \sigma_{ns}^{(3)} = 0$$

and to neglect the terms related to the zero thickness solid. The superscript (2) denoting the fluid medium, one then obtains:

$$\begin{cases} 1) & u_n^{(1)} = U_n^{(2)} \\ 2) & \sigma_{nn}^{(1)} + s^{(1)} = \sigma_{nn}^{(2)} \\ 3) & \sigma_{ns}^{(1)} = 0 \\ 4) & U_n^{(1)} - u_n^{(1)} = 0 \end{cases} \tag{80}$$

In the systems (79) and (80), the tangential displacements are not taken into account as there is no coupling of them between a solid and a fluid. In addition, the obtained relations are identical to those used by Rosenbaum (1974) and Feng and Johnson (1983a, b) although the process had been different (the equation (74) has not been used).

This section could be considered as painstaking, including numerous assumptions not so well warranted. This is the image of reality. Whatever the process is, no demonstration is really satisfactory. It also occurs if the dynamic equations are stated using the macroscopic variables u and $\tilde{\phi}(u - U)$, u being the displacement of the matrix of a continuum (Biot, 1962; Stoll and Bryan, 1970; Dutta and Odé, 1979a, b; Dutta and Odé, 1983; Coussy and Bourbié, 1984). Auriault (1985, personnal communication) proved the pressure continuity of the saturant fluids at the interface between two porous media, using homogenization theory. This result may demonstrate the "power" of such a process.

CHARACTERISTICS OF A SATURATED POROUS MEDIUM.

In this section, the properties of the body wave velocities and attenuations are studied as a function of the saturant fluid, the permeability and the porosity. The parameters given by Rosenbaum (1974) are used for the constitutive grains (K_s and ρ_s) and the skeleton (K_b and μ_b). In addition, the velocities of the solid matrix are considered as the ones of the dry rock (α_m and β_m). Tables 1.1 and 1.2 give all the parameters.

Pore shape: cylindrical ducts

Following homogenization theory, the viscous coupling coefficient $b(\omega)$ and the inertial coupling coefficient $\rho_{22}(\omega)$ can be evaluated for a given pore shape. The classical model of cylindrical ducts with a unidirectional flux (perpendicular to the borehole wall, for instance) is considered. The analytical expression of the complex permeability function $K(\omega)$ is obtained through the evaluation of the flow velocity in a cylindrical duct whose radius is " a " related to the application of a pressure gradient in the case of a motionless solid (the expression is the same when the solid moves). One then obtains (cf., Appendix, after Biot, 1956b and Borne, 1983):

$$K(\omega) = -\frac{\tilde{\phi}}{i\omega\rho_f} \frac{J_2\left[ia\sqrt{\frac{i\omega}{\nu}}\right]}{J_0\left[ia\sqrt{\frac{i\omega}{\nu}}\right]} \tag{81}$$

where

- $\nu = \eta/\rho_f$ is the kinematic viscosity of the fluid
- J_n denote the Bessel functions of the first kind of the n-th order.

The radius a is given by the low frequency limit of $b(\omega)$ which must be compatible with Darcy's law (i.e., $b(0) = \eta\tilde{\phi}^2/\tilde{k}$, see Appendix). The relation (38) is again verified:

$$a^2 = 8\frac{\tilde{k}}{\tilde{\phi}}$$

The expression of $b(\omega)$ deduced from the equation (81) is equivalent to the one of Biot (1956b) with a "structural factor" equal to $\sqrt{8}$. In the high frequency range $b(\omega)$ is proportional to $\omega^{\frac{1}{2}}$.

The low and high frequency limits of the inertial coupling coefficient $\rho_{22}(\omega)$ are (see Appendix):

$$\begin{aligned} \lim_{\omega \to 0} \rho_{22}(\omega) &= \frac{4}{3}\tilde{\phi}\rho_f = \frac{4}{3}\rho_2 \\ \lim_{\omega \to \infty} \rho_{22}(\omega) &= \tilde{\phi}\rho_f = \rho_2 \end{aligned} \tag{82}$$

These relations are again analogous to those of Plona and Johnson, 1980, (see eq. 42). Here the tortuosity θ is frequency dependent.

Discussion

Several assumptions are made when using the cylindrical duct model. The major topics are:

- Using the relation (38) for the pore radius, it is implicitly assumed that it is still valid for the dynamic state although evaluated for the quasi-static state. The real and modeled formations of equal porosity and permeability are considered as equivalent from the point of the dynamic filtration of a given fluid when the relation (38) is verified.

- No relation of the Kozeny-Carman type relating the porosity, the permeability and the pore radius is used (see, for example, Ogushwitz, 1985; Pape et al., 1985) nor any semi-empirical relations. In other respects, these equations are only valid in the quasi-static domain of uniform saturant fluid flow.

- The mass coupling coefficient $\rho_{22}(\omega)$ as well as the viscous coupling coefficient $b(\omega)$ depend only on the pore shape.

The cylindrical duct model with a unidirectional flow implies numerous assumptions. However, it leads to a coherent definition of all parameters for given permeability and porosity. The effects of the pore shape and pore geometry on the dynamic behavior of a saturated porous medium are investigated in Part III of this study. It has to be mentioned that the pore models do not change the *relative variations* of the medium behavior related to permeability, porosity or saturant fluid properties modification.

Coupling coefficients and body waves

The formation used is a Berea sandstone (see Table 1.1). The calculations are made in the frequency range [1, 10^7] Hz. The mass coupling coefficient, $\rho_{22}(\omega)$ and the viscous

coefficient $b(\omega)$) are given in a nondimensional form:

$$\begin{aligned} \rho_{22}^*(\omega) &= \frac{\rho_{22}(\omega)}{\rho_2} \\ b^*(\omega) &= b(\omega)/\left(\frac{\eta\tilde{\phi}^2}{\tilde{k}}\right) \end{aligned} \tag{83}$$

Following Dutta and Odé (1983), the body wave (P_1, P_2, S) attenuations are given in decibels per wavelength. Denoting k_j the wavenumber related to a body wave:

$$k_j = \frac{\omega}{c_j(\omega)} + i\gamma_j \quad j = 1, 2, 3 \tag{84}$$

where

- c_j is the phase velocity (α_1, α_2, β)
- γ_j is the attenuation coefficient.

The attenuation in dB/λ (or dB/Hz-sec) is given by:

$$A_j = 8.686\,\frac{\gamma_j c_j}{f} = 27.286 \times \frac{2\gamma_j c_j}{\omega} \tag{85}$$

This value is proportional to the inverse of the quality factor Q_j. When $Q_j \gg 1$, the following classical relation is verified:

$$A_j = \frac{27.286}{Q_j} \tag{86}$$

The attenuation coefficient will be given in dB/m.

The phase velocities are dispersive. The group velocities g_j are numerically evaluated using the fact that at the low frequency limit $g_1 = \alpha_1$; $g_2 = 2\alpha_2$; $g_3 = \beta$ and that at the high frequency limit $g_j = c_j$, j = 1,2,3 (see Boutin, 1983).

Saturant fluid effects

Besides the pore shape, the saturant fluid properties affect both velocity and attenuation of the body waves. In the following, the porosity is 19 % and the permeability is equal to 200 md. To begin with, only "homogeneous" saturant fluids are considered: heavy oil (1), water (2) and gas (3) (see Table 1.2). The characteristic frequency is very high for heavy oil ($\cong$ 31360 kHz). The coupling coefficients are then almost constant in the whole frequency range ($\rho_{22}^*(\omega) = 4/3$; $b^*(\omega) = 1$, Figure 2a). In the cases of water and gas saturations, they depart from the static values for a frequency around $f_c/8$. This

is due to the expression of the argument of the complex permeability function which includes the pore radius. As previously stated, $b^*(\omega)$ is then proportional to $\sqrt{\omega}$ and $\rho_{22}^*(\omega)$ tends to 1.

The nature of the saturant fluid modifies the wave velocities of the porous medium (Figure 2b). In the low frequency range, the distribution is:

$$\begin{aligned} \alpha_{1G} &< \alpha_{1O} < \alpha_{1W} \\ \beta_O &< \beta_W < \beta_G \end{aligned}$$

(G = gas; O = oil; W = water)

while for Poisson's ratio:

$$\nu_G < \nu_O < \nu_W$$

As indicated by the scale of the figures, the dispersion is rather weak for the P_1 and S waves. It occurs in correlation with the disconnecting of the coupling coefficients (i.e., for $f \cong f_c/8$). The characteristic frequency is underlined by the first inflexion point of the group velocities. The low and high frequency expressions for the S wave are easy to evaluate analytically (see Schmitt, 1985, for example):

$$\lim_{\omega \to 0} \beta^2 = \frac{(1-\tilde{\phi})\rho_s \beta_m^2}{(1-\tilde{\phi})\rho_s + \tilde{\phi}\rho_f} \tag{87}$$

$$\lim_{\omega \to \infty} \beta^2 = \frac{N}{\rho_{11} - \dfrac{\rho_{12}^2}{\rho_{22}}} \tag{88}$$

The relation (87) explains the velocity distribution as a function of the saturant fluid. However, only its density plays a part: the greater it is, the lower the S wave velocity is.

The equation (88) is general. With the unidirectional cylindrical ducts model , it becomes:

$$\lim_{\omega \to \infty} \beta^2 = \beta_m^2 \tag{89}$$

which is independent of the porosity and the saturant fluid.

The behavior of the slow P_2 wave is completely different. The phase velocity is very dispersive: nearly equal to zero for very low frequencies, it tends to the saturant P wave velocity (within 10%). This corresponds to the limit indicated by Plona and Johnson (1980). The first horizontal tangent of the group velocity occurs at $f = f_c/8$.

Looking at the P_1 and S wave attenuations (Figures 2c, 2d), the "low frequency" range, for which the viscous forces are dominant, is clearly separated from the "high

frequency" range for which the inertial forces are no longer negligible. The limit corresponds to the *critical frequency* of the porous media as given by the equation (32) i.e.:

$$f_{ci} = \frac{b}{2\,\pi\,\rho_{22}}$$

Neglecting the variations of $b(\omega)$ and $\rho_{22}(\omega)$ yields:

$$f_{ci} = \frac{\eta\tilde{\phi}^2}{2\pi\tilde{k}\rho_{22}(0)} = \frac{3}{4}\,f_c \tag{90}$$

Each of these ranges is characterized by a frequency dependence:

$$\begin{cases} f < f_{ci} & A_{P_1}(Q_{P_1}^{-1}) \propto f & \gamma_{P_1} \propto f^2 \\ & A_S(Q_S^{-1}) \propto f & \gamma_S \propto f^2 \\ f > f_{ci} & A_{P_1}(Q_{P_1}^{-1}) \propto f^{-\frac{1}{2}} & \gamma_{P_1} \propto f^{\frac{1}{2}} \\ & A_S(Q_S^{-1}) \propto f^{-\frac{1}{2}} & \gamma_S \propto f^{\frac{1}{2}} \\ f = f_{ci} & A_{P_1}(Q_{P_1}^{-1}) \text{ and } A_S(Q_S^{-1}) & \text{are maximum} \end{cases} \tag{91}$$

Whatever the saturant fluid is, the S wave attenuation is greater than the P_1 wave attenuation. The difference increases from gas to water saturation.

Contrary to what is generally stated, the P_1 and S wave attenuations are not characteristic of the saturant fluid in the whole frequency range.

Below the critical frequency relative to the gas saturation case (i.e., $\cong$ 18 kHz), the "usual" distribution occurs:

$$\begin{array}{lcl} A_{P_1}(G) > A_{P_1}(W) & > & A_{P_1}(O) \\ A_S(G) \cong A_S(W) & > & A_S(O) \end{array} \tag{92}$$

It is identical for the attenuation coefficient.

Up to its critical frequency ($\cong$ 114 kHz), the water saturated porous medium is the most attenuating one. Beyond this value, the heavy oil leads to the greatest attenuation.

Although the "low frequencies" practically correspond to the application ranges of the varied exploration techniques, one should not make any generalization. In addition to the saturant fluid viscosity, its compressibility plays a part in energy dissipation related to the fluid-solid differential motion.

Finally, the attenuations shown in these cases are relatively weak, especially for the P_1 wave.

Below the critical frequency f_{ci}, the P_2 wave is quasi diffusive. Whatever the saturant is, its attenuation A_{P_2} is equal to 54.6 dB. Beyond this value, it decreases as $f^{-\frac{1}{2}}$.

Contrary to the P_1 and S waves, the attenuation coefficient is always proportional to the square root of the frequency. The relations (91) have to be completed by:

$$\begin{cases} f < f_{ci} & A_{P_2} \cong 54.6\,\text{dB} & \gamma_{P_2} \propto f^{\frac{1}{2}} \\ f > f_{ci} & A_{P_2} \propto f^{-\frac{1}{2}} & \gamma_{P_2} \propto f^{\frac{1}{2}} \end{cases} \tag{93}$$

In the low frequency range, the saturant fluid is characterized only through the attenuation coefficient variations:

$$\gamma_{P_2}(O) > \gamma_{P_2}(W) > \gamma_{P_2}(G) \tag{94}$$

Despite the title of this section, only the absolute variations of the different attenuations have been shown. Only some trends, related to the nature of the saturant fluid, have been pointed out. Even if, following Biot (1956b), it is assumed that the energy dissipation can be characterized by a function D equal to $\frac{1}{2}b(\dot{u}_i - \dot{U}_i)(\dot{u}_i - \dot{U}_i)$, no general rules related only to fluid viscosity can be established.

The study of "inhomogeneous" fluids (i.e., mixtures) may show the complexity of the phenomenon. To do so, the bulk parameters of the resulting fluid are necessary.

Domenico (1977) quantifies the effects of gas presence in water through the density (ρ) and the compressibility (C):

$$\begin{aligned} \rho_f &= S_W \rho_W + (1 - S_W)\rho_G \\ C_f &= S_W C_W + (1 - S_W)C_G \end{aligned} \tag{95}$$

where

- the subscripts f, W, G denote the resulting fluid, the water and the gas,
- S_W is the water saturation degree of the fluid.

These formulas implicitly asssume that the water and the gas are mixed in the same proportions everywhere in the pore space. In addition, laboratory experiments (Foster Allen et al., 1980) showed that a 10% presence of air reduces the compressional wave velocity in the water by about a quarter. At this value, there are a small number of gas bubbles in the water. Dutta and Odé (1979a, b) have analyzed the attenuation and dispersion of compressional waves in fluid filled porous rocks with partial gas saturation. They used White's model (1975) and the classical Biot's theory in the low frequency range since their work concerned the seismic exploration band, i.e. 10-150 Hz. It cannot be therefore directly applied to the high frequency domain and to the well logging situation. Arditty (1978) also changes the viscosity in accordance with practical tables (Carr et al., 1954; Standing and Katz, 1942a, b).

Cases of water-gas mixtures are studied in the following section. The velocities and attenuations are relative to:

- pure water (1)
- "gaseous water" (2). Only the compressional wave velocity is lowered (α = 800 m/s). The coupling coefficients, the critical and characteristic frequencies are then identical to those of pure water (see Figure 3.a)
- "gaseous water" (3) for which the velocity, the density and the viscosity have been changed following Arditty (1978) (see Table 1.2). The coupling coefficients are then less than those of pure water. The compressibility and the critical frequency are less than those of the previous case.
- pure gas (4)

In the low frequency range (Figure 3b), the P_1 velocity of the mixtures is less than the P_1 velocity of the pure gas saturation. The more compressible the mixture is, the lower the P_1 wave velocity is. This result, which may be surprising, is mentioned by Toksöz et al. (1976). It has been obtained from measurements or calculations using the Toksöz et al. model, under some confining pressure conditions. In the very high frequency range, greater than all the critical frequencies, the velocities are distributed as the decreasing compressiblities of the saturant fluids. This is due to a greater dispersion for the "gaseous waters". At intermediate frequencies, various situations can occur.

The modifications and the variations of the shear wave velocities are simpler and identical in the whole frequency range. In accordance with the equations (87) and (88), *only the saturant fluid density* plays a role. The distribution is: $\beta(1) = \beta(2) < \beta(3) < \beta(4)$. This order differs from the P_1 wave relations. Poisson's ratio is thus changed.

At very high frequencies, the P_2 velocities are proportional to those of the saturant fluids. At intermediate frequencies, the situation is complex, strongly influenced by the critical frequencies. In the low frequency range, the distribution is $\alpha_2(4) > \alpha_2(3) > \alpha_2(1) > \alpha_2(2)$.

The distribution of the attenuations in dB/λ and dB/m of the P_1 and S waves (Figures 3c, 3d) is simple only for frequencies less than the gas critical frequency. In this "low frequency" range, the first effect of the fluid velocity decrease is a greater attenuation of the P_1 waves, nearly equal to that of gas despite the viscosity ratio ($\cong$ 45). With similar compressibilities, an increase in the viscosity (on the order of 5) leads to much greater P_1 and S wave attenuations. These are greater than those obtained with the gas which is, however, more compressible and less viscous. To summarize, the distribution is:

$$\begin{aligned} A_{P_1}(3) > A_{P_1}(4) \quad &\geq A_{P_1}(2) > A_{P_1}(1) \\ A_S(3) > A_S(2) \quad &= A_S(1) \geq A_S(4) \end{aligned}$$

and likewise for the attenuation coefficients.

Correlatively, the maxima associated with the critical frequencies are greater for the mixtures, all the more when the saturant fluid is less compressible. It has to be noted that a simple decrease of the saturant fluid velocity does not change the S wave velocity and attenuation or the critical frequency of the porous medium.

As for the "homogeneous" fluids, the variations of the attenuation in decibels per wavelength of the slow P_2 wave only show the modifications of the critical frequencies. In the "high frequency" range, the distribution is then:

$$A_{P_2}(4) < A_{P_2}(3) < A_{P_2}(1) \cong A_{P_2}(2)$$

The attenuation coefficients are distributed in the reverse order of the "low frequency" velocities, i.e.:

$$\gamma_{P_2}(4) < \gamma_{P_2}(3) < \gamma_{P_2}(1) < \gamma_{P_2}(2)$$

For equal viscosity, the more compressible the fluid is the greater the resistance to the flow. Inversely, for similar compressibilities, the lower the viscosity is the greater the relative motion between the two phases. The P_2 wave is thus more propagative and less dissipative. This result is still true when the viscosity *and* the compressibility are lowered.

In the case of the oil-gas mixture, whatever the body wave (P_1, P_2 or S), the relative variations of the velocities and attenuations are identical to the ones just described.

It is thus only for the "low" frequencies that the saturant fluid nature can be *approached* using only the characteristics of the P_1 and S waves: velocities (i.e., Poisson's ratio) and attenuations. One has to be aware of any extreme generalization, especially for porous media saturated by mixtures.

Permeability effects

For a porosity of 19% and a given saturant fluid, the body wave velocities and attenuations are evaluated for different permeabilities: 2 md, 32.5 md, 200 md, 500 md, 1 darcy, 1.5 d and 5 d (respectively (1), (2), (3), (4), (5), (6) and (7) in Figures 4a, b, c, d and 5a, b, c and d).

Whatever the saturant fluid, an increase in the permeability leads to a decrease of the critical frequency (see eq. 89) and of the quasi-static value of the viscous coupling coefficient. At the same time, the pore radius (a) increases. The relative motion between the two phases is then enhanced. The densities per unit volume of the porous medium (i.e., ρ_1 and ρ_2) remain unchanged. This is also true for the low and high frequency limits of the mass coupling coefficient and the density of the medium (see Figures 4.a and 5.a for the water and gas saturations, respectively).

As one could infer from the equations (87) and (88) for the S wave, a permeability

increase has no effect upon the absolute values of the body wave velocities (Figures 4b; 5b). The shift toward low frequency of the critical frequency results in a lower frequency occurrence of the noticeable dispersion.

The greater the permeability, the more important the relative motion between the two phases and thus the two phase character of the porous medium. This leads to an increase in the P_1 and S wave energy dissipation (Figures 4c, 4d; 5c, 5d). However, because of the discontinuity in slope of the attenuations around the critical frquency, this characteristic is only valid in the quasi-static range. At best, it is true for frequencies lower than the critical frequency relative to the highest permeability. This limitation is all the more drastic in that the maximum of attenuation in decibels per wavelength is identical. Physically, this is because the mass coupling coefficient $\rho_{22}(\omega)$ remains unchanged. The curves are then just shifted toward the low frequencies when the permeability increases.

Depending on the frequency range considered, the measurement of the P_1 and S wave attenuations are not always representative of the medium permeability. As a matter of fact, it is only for a uniform flow that the determinations will not be ambiguous.

The slow P_2 wave becomes propagative at lower frequencies in correlation with the critical frequency decrease and its attenuation coefficient is inversely proportional to the permeability. This wave is then representative of the permeable character of a saturated porous medium.

Porosity effects

The porosity is a critical parameter in the sense that it governs the mechanical properties of the porous medium (velocities and density) as well as the critical frequency.

Several authors use expressions relating the porosity to the skeleton bulk modulus (K_b). For example, Ogushwitz (1985), after Hamilton (1976), gives:

$$\log K_b = x - y\tilde{\phi}$$

where x and y are constants which depend on the rock and constitutive materials.

K_b can also be evaluated using the "Toksöz model" (Kuster and Toksöz, 1974 a, b; Cheng and Toksöz, 1979; Toksöz et al., 1976) or the Berryman (1980) model (see Ogushwitz, 1985).

Semi-empirical formulas also exist. For example, Raymer et al. (1980) give for the consolidated rocks, i.e. $\tilde{\phi} < 35\%$:

$$V = (1 - \tilde{\phi})^2 V_m + \tilde{\phi} V_f$$

while for $\tilde{\phi} > 45\%$:

$$\frac{1}{\rho V} = \frac{\tilde{\phi}}{\rho_f V_f^2} + \frac{1-\tilde{\phi}}{\rho_m V_m^2}$$

where the subscripts f and m denote the saturant fluid and the matrix, respectively.

In this paper, the dry rock velocities are kept constant. K_b varies in accordance to the equation (17). In the following examples, the porosity values are 5%, 8%, 10%, 19% and 30% (cases (1), (2), (3), (4), (5) respectively). The permeability is equal to 200 millidarcies. Figure 6a shows the normalized coupling coefficients for the water saturation situation.

Within the quasi-static range, when the porosity increases the P_1 and S wave velocities decrease, but not at the same rate (Figure 6b). The Poisson's ratio also decreases. At the same time, the dispersion is more important. The high frequency limit of the S wave velocity is identical for each porosity because of the way the calculations are done and the chosen pore shape model. The P_1 velocities, on the contrary, increase with decreasing porosity.

The behavior of the P_2 wave is identical for the low frequencies but the distribution is reversed for the high frequency limit. The smaller the porosity, the less important the fluid volume. The P_1 and S wave attenuations are then weaker (Figures 6c, 6d). As the critical frequency varies with the porosity, the attenuation curves are simply shifted along the x and y axis. The shear wave attenuations in the quasi-static range are very close to one another. The differences are only clear around the critical frequencies and beyond these values. Lastly, whatever the porosity is, the S wave attenuation is greater than the P_1 wave attenuation. The difference decreases inversely with porosity.

As with permeability, the attenuation coefficients of the slow P_2 wave follow the distribution of the viscous coupling coefficient. The smaller the porosity, the less important they are.

The general trends still behave for the gas saturation situation. Only a few differences occur. They are related, for example, to the difference between the P_1 and S wave attenuations (see Schmitt, 1985).

The porosity effects, contrary to permeability, cannot be inferred from the viscous coupling coefficient and the critical frequency alone.

A porosity increase leads to an increase of:

- the critical frequency
- the viscous coupling coefficient

- the mass coupling coefficient
  and, above all,
- *the moving fluid volume*

It is because of this last feature that the P_1 and S wave attenuations increase while the P_2 attenuation decreases: the porous medium is more diphasic.

As with porosity, the velocities of the dry rock modify the maxima of attenuation of the P_1 and S waves as well as the attenuation coefficient of the slow P_2 wave. They also affect the difference between the attenuations of the two "fast" body waves (see Schmitt, 1985).

CONCLUSION

The constitutive equations of a saturated porous media can be obtained through the use of mixtures theory. Although axiomatic, this formulation emphasizes several assumptions which are not explicit in Biot's papers. It leads to a frequency dependence of the mass coupling coefficient.

Besides this frequency dependence, homogenization theory leads to a somewhat unified definition of the viscous and mass coupling coefficients. They are related to one another through a complex permeability function. This function can be computed for a given pore geometry by integration of the Navier-Stokes equations.

The continuity equations at different kinds of interfaces (porous/porous, porous/solid, porous/fluid)can be inferred from the general principles of mechanics but are not so well proven as one might believe. With several assumptions, the same equations as Deresiewickz and Skalak (1963) have been derived. The uniqueness of the wavefield is then ensured.

Using the formulation previously described, and considering the pores as cylindrical ducts with a unidirectional flow, the properties of the three body waves have been analyzed.

The practical results of that study may be summarized as follows:

- The *critical* frequency of a saturated porous medium is inversely proportional to the low frequency limit of the mass coupling coefficients ρ_{22}. It fixes the frequency for which the attenuations, i.e. the inverse of quality factors, of the P_1 and S waves are maximum. However, the dynamic behavior of a saturated medium occurs at lower frequencies, around the *characteristic* frequency, in correlation with the propagative character of the slow P wave related to a non uniform flow.

- The frequency dependence of the body wave attenuations (see eqn. 91 and 93) are general.
  Because of the "breaking point" in the attenuation variations of the P_1 and S waves, one has to be aware of any general and *a priori* classification concerning the saturant fluid nature and permeability effects that is *independent of the frequency.*

- The maxima of attenuations (in dB/λ) of the P_1 and S waves are independent of the permeability for a given formation, a given saturant fluid and a given porosity.

- It is only in the low frequency range (i.e., below the critical frequencies) that a permeability increase leads to an increase of the P_1 and S wave attenuations.

- The P_1 and S wave attenuations increase with the porosity for a given formation, a given saturant fluid, and a given permeability.

- The slow P_2 wave is inhomogeneous, especially in the low frequency range. Its characteristics strongly depend, for given permeability and porosity, on the saturant fluid mobility. This last parameter is a function of the compressibility and the viscosity of the liquid. Its phase velocity is always less than the P wave velocity of the pore fluid. Therefore, in the borehole configuration, this wave cannot be critically refracted at the borehole wall, thus it cannot be recorded.

ACKNOWLEDGEMENTS

I am indebted to Dr. G. Bonnet and Prof. J.L. Auriault for many valuable and helpful discussions. I would like to thank Prof. M.N. Toksöz, Dr. C.H. Cheng and Dr. R.H. Wilkens for constructive and stimulating comments on this manuscript. This work was supported by the Société Nationale Elf Aquitaine (Production) and the Centre de Calcul Vectoriel pour la Recherche.

REFERENCES

Aki, K., and Richards, P.G., 1980, Quantitative seismology. Theory and methods, W.H. Freeman and Co. San Francisco.

Arditty, P.C., 1978, The earth tide effects on petroleum reservoirs. Engineer Degree, Stanford Univ.

Auriault, J.L., 1980, Dynamic behaviour of a porous medium saturated by a newtonian fluid. Int. J. Eng. Sci., 18, 775-785.

————, 1981, Homogenization. Application to porous saturated media.In *Two Medium Mechanics*, Summer School, Gdansk, 5-9 September.

Auriault, J.L., Borne, L., and Chambon, R., 1985, Dynamics of porous saturated media, checking of the generalized law of Darcy. J. Acoust. Soc. Am., 77, 1641-1650.

Avallet, C.,1981, Comportement dynamique de milieux poreux saturés. These D.I. Grenoble Univ.

Berryman, J.G., 1980a, Long-wavelength propagation in composite elastic media. I. Spherical inclusions. J. Acoust. Soc. Am.,68, 1809-1819.

————, 1980b, Long wavelength propagation in composite elastic media. II. Ellipsoidal inclusions. J. Acoust. Soc. Am., 68, 1820-1831.

————, 1980c, Confirmation of Biot's theory. Appl. Phys. Letters, 37 , 382-384.

Biot, M.A., 1956a, Theory of propagation of elastic waves in a fluid saturated porous solid. I. Low frequency range. J. Acoust. Soc. Am., 28, 168-178.

———, 1956b, Theory of propagation of elastic waves in a fluid saturated porous solid. II. Higher frequency range. J. Acoust. Soc. Am., 28, 179-191.

———, 1962, Mechanics of deformation and acoustic propagation in porous media. J. Appl. Phys., 33, 1482-1488.

Bonnet, G., 1985, Contribution à l'étude des milieux poreux saturés en régime dynamique. Thèse d'Etat. Montpellier Univ.

Borne, L., 1983, Contribution à l'étude du comportement dynamique des milieux poreux saturés déformables. Etude de la loi de filtration dynamique. Thèse D.I. Grenoble Univ.

Boutin, C., 1983, Contribution à l'étude du comportement dynamique des milieux poreux. D.E.A. Grenoble Univ.

Brown, R.J.S., 1980, Connection between formation factor for electrical resistivity and fluid-solid coupling factor in Biot's equation for acoustic waves in fluid filled porous media. Geophysics, 45, 1269-1275.

Carr, N.J., Kobayashi, R., and Burrow, D.B., 1954, Viscosity of hydrocarbon gases under pressure. Trans. AIME, 201.

Cheng, C.H., and Toksöz, M.N., 1979, Inversion of seismic velocities for the pore aspect ratio spectrum of a rock. J. Geophys. Res., 84, 7533-7543.

Coussy, O.,and Bourbié, T., 1984, Propagation des ondes acoustiques dans les milieux poreux. Revue de l'IFP.1.

Deresiewickz, H.,and Skalak, R., 1963, On uniqueness in dynamic poroelasticity. Bull. Seism. Soc. Am., 53, 783-788.

Domenico, S.N., 1977, Elastic properties of unconsolidated porous sand reservoirs. Geophysics, 42, 1339-1368.

Dutta, N.C., 1980, Theoretical analysis of observed second bulk compressional wave in a fluid saturated porous solid at ultrasonic frequencies. Appl. Phys. Lett., 37, 898-900.

Dutta, N.C., and Odé, H., 1979a, Attenuation and dispersion of compressional waves in fluid filled porous rocks with partial gas saturation (White model). I. Biot's theory. Geophysics, 44, 1777-1788.

———————, 1979b, Attenuation and dispersion of compressional waves in fluid filled porous rocks with partial gas saturation (White model). II. Results. Geophysics, 44, 1789-1805.

———————, 1983, Seismic reflections from a gas water contact. Geophysics, 48, 148-162.

Feng, S., and Johnson, D.L., 1983 a, High frequency acoustic properties of a fluid/porous interface. I. New surface mode. J. Acoust. Soc. Am., 74, 906-914.

———————, 1983 b, High frequency acoustic properties of a fluid/porous interface. II. The 2D reflection Green's function. J. Acoust. Soc. Am., 74, 915-925.

Foster Allen, N., Richart, F.E., and Woods, R.D., 1980, Fluid wave propagation in saturated and nearly saturated sands. J. Geoth. Eng. Div. , 106, 235-254.

Hamilton, E.L., 1976, Elastic properties of marine sediments. J. Geophys. Res., 76, 579-604.

Johnson, D.L., Plona, T.J., Scala, C., Pasierb, F., and Kojima, F., 1982 , Tortuosity and acoustic slow waves. Phys. Rev. Lett., 49, 1840-1844.

Kuster, G.T., and Toksöz, M.N., 1974a, Velocity and attenuation of seismic waves in two phase media. I. Theoretical formulation. Geophysics, 39, 587-606.

————————, 1974b, Velocity and attenuation of seismic waves in two phase media. II. Experimental results. Geophysics, 39, 607-618.

Landau, L., and Lifschitz, E., 1971, Mecanique des fluides. Ed. Mir. Moscou.

Mavko, G.M., and Nur, A., 1979, Wave attenuation in partially saturated rocks. Geophysics, 44, 161-178.

Ogushwitz, P.A., 1985a, Applicability of the Biot's theory. I. Low porosity materials. J. Acoust. Soc. Am., 77, 429-440.

————, 1985b, Applicability of the Biot's theory. II. Suspensions. J. Acoust. Soc. Am., 77, 441-452.

————, 1985c, Applicability of the Biot's theory. III. Wave speeds versus depth in marine sediments. J. Acoust. Soc. Am., 77, 453

Pape, H., Riepe, L., and Schopper, J.R., 1985, Permeability of porous rocks derived from internal surface effects. 47-th EAEG Int. Meet., Budapest.

Plona, T.J., 1980, Observation of a second bulk compressional wave in a porous medium at ultrasonic frequencies. Appl. Phys. Lett., 36, 259-261.

Plona, T.J., and Johnson, D.L., 1980, Experimental study of the two bulk compressional modes in water saturated porous structures. Ultrasonic Symposium, 864-872.

Ramey, L.L., Hunt, E.R., and Gardner, J.S., 1980, An improved source transit time to porosity transform. 21-st SPWLA Ann. Logg. Symp.

Rosenbaum, J.H., 1974, Synthetic microseismograms: logging in porous formations. Geophysics, 39, 14-32.

Schmitt, D.P., 1985, Simulation numérique de diagraphies acoustiques. Propagation d'ondes dans des formations cylindriques axisymétriques radialement stratifiées incluant des milieux élastiques et/ou poreux saturés. Ph.D. thesis. Grenoble Univ.

Sen, P.N., Scala, C., and Cohen, M.H., 1981, A self-similar model for sedimentary rocks with application to the dieletric constant of fused glass beads, Geophysics, 46, 781-795.

Standing, M.B., and Katz, D.L., 1942a, Density of crude oils saturated with natural gas, Trans. AIME, 146, 159-161.

————————————,1942b, Density of natural gases. Trans. AIME, 146, 190-191.

Stoll, R.D., and Bryan, G.M., 1970, Wave attenuation in saturated sediments. J. Acoust. Soc. Am., 47, 1440-1447.

Toksöz, M.N., Cheng, C.H., and Timur, A., 1976, Velocities of seismic waves in porous rocks. Geophysics, 41, 621-645.

Truesdell, C., and Toupin, R., 1960, Handbuck der Physick; vol. III/1, Springler Verlag. Ed. Berlin.

White, J. E., 1975, Computed seismic speed and attenuation of rocks with partial gas saturation. Geophysics, 40, 224-234.

APPENDIX

COUPLING COEFFICIENTS FOR CYLINDRICAL DUCTS

Evaluation of the complex permeability function

The analytic expression of the complex permeability function $K(\omega)$ is obtained through the evaluation of the flow velocity in a cylindrical duct whose radius is " a " related to the application of a pressure gradient in the case of a motionless solid (the expression is the same when the solid moves). The developments thereafter follow Biot's (1956b) and Borne's (1983) presentations.

A pressure gradient is applied along x (see Figure A1) which is the flow direction. The flux is assumed to be axisymmetric and $\vec{U}$ is considered to be independent of x. The equation of motion of a viscous Newtonian liquid in the x direction may be written:

$$\rho_f \ddot{U} = -\frac{\partial P}{\partial x} + \eta \nabla^2 \dot{U} \tag{A.1}$$

where P denotes the pressure and η the dynamic viscosity of the fluid.

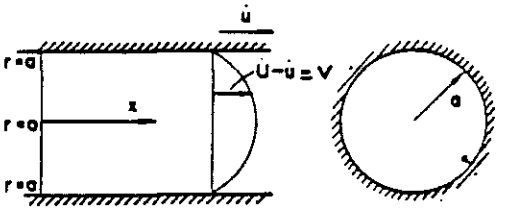

(from Biot, 1956 b)

Setting $F = -\frac{\partial P}{\partial x}$, equation (A.1) becomes (for a moving solid, one needs to put down $v = \dot{U} - \dot{u}$ and $F = -\frac{\partial P}{\partial x} - \rho_f \ddot{u}$, see Biot, 1956b):

$$\eta \nabla^2 v + F = \rho_f \dot{v} \tag{A.2}$$

Because of the axial symmetry $v = v(r)$, and assuming a temporal dependence $e^{i\omega t}$, the equation may be written:

$$\frac{d^2 v}{dr^2} + \frac{1}{r}\frac{dv}{dr} - \frac{i\omega\rho_f}{\eta} v = -\frac{F}{\eta} \tag{A.3}$$

This is a Kelvin's equation whose solution is (v has to remain finite when $r = 0$):

$$v(r) = \frac{1}{i\omega\rho_f} F \left[1 - \frac{J_0\left\{ ir\sqrt{\frac{i\omega}{\nu}} \right\}}{J_0\left\{ ia\sqrt{\frac{i\omega}{\nu}} \right\}} \right] \tag{A.4}$$

where

- $\nu = \eta/\rho_f$ is the kinematic viscosity of the fluid,
- J_0 is the Bessel function of the first kind of the zero-th order.

The hydraulic permeability $K(\omega)$ is then given by:

$$K(\omega) = \frac{2\tilde{\phi}}{a^2} \int_0^a \frac{v(r)}{F} r\, dr \tag{A.5}$$

where

- F is a constant in relation to r
- $\tilde{\phi}$ is the porosity

Then, using the recurrence relations of the Bessel functions:

$$\begin{aligned} \frac{d(z^n J_n(z)}{dz} &= z^n J_{n-1}(z) \\ \frac{2n}{z} J_n(z) &= J_{n-1}(z) + J_{n+1}(z) \end{aligned}$$

one obtains:

$$K(\omega) = -\frac{\tilde{\phi}}{i\omega\rho_f} \frac{J_2\left\{ia\sqrt{\frac{i\omega}{\nu}}\right\}}{J_0\left\{ia\sqrt{\frac{i\omega}{\nu}}\right\}} \tag{A.6}$$

Low frequency range

For a complex z, :

$$\begin{aligned} \lim_{z\to 0} J_n(z) &= \left(\frac{1}{2}z\right)^n \sum_{k=0}^{\infty} \frac{\left(-\frac{1}{4}z^2\right)^k}{k!\,\Gamma(n+k+1)} \\ &= \left(\frac{1}{2}z\right)^n \sum_{k=0}^{\infty} \frac{\left(-\frac{1}{4}z^2\right)^k}{k!\,(n+k)!} \end{aligned} \tag{A.7}$$

Substituting $z = ia\sqrt{\frac{i\omega}{\nu}}$ yields:

$$\begin{aligned}\lim_{z\to 0}\frac{J_0(z)}{J_2(z)} &\cong \frac{8i\nu}{a^2\omega}\,\frac{1+\frac{i}{4}\frac{a^2\omega}{\nu}-\frac{a^4\omega^2}{64}\nu^2}{1+i\frac{a^2\omega}{12\,\nu}} \\ &\cong \frac{8i\nu}{a^2\omega}\left[1-\frac{a^4\omega^2}{64\,\nu^2}+\frac{i}{4}\frac{a^2\omega}{\nu}\right]\left[1-\frac{a^4\omega^2}{144\,\nu^2}-i\frac{a^2\omega}{12\,\nu}\right] \\ &\cong -\frac{4}{3}+i\left[\frac{8\nu}{a^2\omega}+\frac{a^2\omega}{24\,\nu}\right]\end{aligned} \tag{A.8}$$

so that,

$$\begin{aligned}\lim_{\omega\to 0} H(\omega) &= \lim_{\omega\to 0}\frac{1}{K(\omega)} = \lim_{\omega\to 0}(\,H_1(\omega)+i\,H_2(\omega)) \\ &= -\frac{i\omega\rho_f}{\tilde{\phi}}\left[\frac{4}{3}+i\left(\frac{8\nu}{a^2\omega}+\frac{a^2\omega}{24\,\nu}\right)\right]\end{aligned} \tag{A.9}$$

Using the relations (41), one obtains:

$$\lim_{\omega\to 0} b(\omega) = \lim_{\omega\to 0}\tilde{\phi}^2\,H_1(\omega) = \frac{8\eta\tilde{\phi}}{a^2} \tag{A.10}$$

$$\lim_{\omega\to 0}\rho_{22}(\omega) = \lim_{\omega\to 0}\frac{\tilde{\phi}^2\,H_2(\omega)}{\omega} = \frac{4}{3}\tilde{\phi}\rho_f = \frac{4}{3}\rho_2 \tag{A.11}$$

The compatibility with Darcy's law enforces:

$$\frac{\eta\tilde{\phi}^2}{\tilde{k}} = \frac{8\eta\tilde{\phi}}{a^2} \quad \text{i.e.,} \quad \tilde{k} = a^2\frac{\tilde{\phi}}{8} \tag{A.12}$$

where $\tilde{k}$ is the medium permeability. This is again the relation (38).

High frequency range

For a complex z:

$$\begin{aligned}\lim_{z\to\infty} J_n(z) = \sqrt{\frac{2}{\pi z}}\,\Big(\quad &\cos(z-\frac{\pi n}{2}-\frac{\pi}{4})\left[1-\frac{(4n^2-1)(4n^2-9)}{128\,z^2}\right] \\ &-\sin(z-\frac{\pi n}{2}-\frac{\pi}{4})\left[\frac{4\lambda^2-1}{8z}\right]\Big)\end{aligned}$$

Using the same notations as previously:

$$\lim_{z\to\infty}\frac{J_0(z)}{J_2(z)} = -\frac{1+\frac{1}{8z}\tan(z-\frac{\pi}{4})}{1-\frac{15}{8z}\tan(z-\pi-\frac{\pi}{4})} \tag{A.13}$$

then

$$\begin{aligned} z &= i\,a\sqrt{\frac{i\omega}{\nu}} = i\,(i+1)\,a\sqrt{\frac{\omega}{2\nu}} \\ z &= (i-1)\,\alpha \end{aligned} \tag{A.14}$$

so that,

$$\begin{aligned} \sin z &= i\,\sinh\alpha\,\cos\alpha - \sin\alpha\,\cosh\alpha \\ \cos z &= \cosh\alpha\,\cos\alpha + i\,\sin\alpha\,\cosh\alpha \end{aligned} \tag{A.15}$$

When $\omega\to\infty$, $z\to\infty$, $\alpha\to\infty$, the above expressions become:

$$\begin{aligned} \sin z &\cong \frac{e^{\alpha}}{2}\,(-\sin\alpha + i\,\cos\alpha) \\ \cos z &\cong \frac{e^{\alpha}}{2}\,(\cos\alpha + i\,\sin\alpha) \end{aligned}$$

so that,

$$\tan z = \frac{i-\tan\alpha}{i\,\tan\alpha+1} \tag{A.16}$$

Then

$$\lim_{\omega\to\infty}\tan z = \lim_{\omega\to\infty}\tan(z-\frac{\pi}{4}) = \lim_{\omega\to\infty}\tan(z-\pi-\frac{\pi}{4}) = i \tag{A.17}$$

The relations (A.13) may thus be written:

$$\begin{aligned} \lim_{z\to\infty}\frac{J_0(z)}{J_2(z)} &\cong -\frac{1-\frac{i}{8z}}{1-i\frac{15}{8z}} \\ &\cong -\left[1+\frac{2i}{z}\right] \end{aligned} \tag{A.18}$$

so that

$$\begin{aligned} \lim_{\omega\to\infty} H(\omega) &= \frac{i\omega\rho_f}{\tilde{\phi}}\left[1+\frac{2}{a}\sqrt{\frac{\nu}{i\omega}}\right] \\ &= \frac{i\omega\rho_f}{\tilde{\phi}}\left[1+\frac{2}{a}(1-i)\sqrt{\frac{\nu}{2\omega}}\right] \end{aligned}$$

Then,

$$\lim_{\omega\to\infty} b(\omega) = \frac{2\tilde{\phi}}{a}\sqrt{\frac{\eta\omega\rho_f}{2}} = X\omega^{\frac{1}{2}} \tag{A.19}$$

$$\lim_{\omega\to\infty}\rho_{22}(\omega) = \tilde{\phi}\rho_f\,(1+\frac{2}{a}\sqrt{\frac{\eta\rho_f}{2\omega}}) \tag{A.20}$$

TABLES

Physical parameters used in this study

1.1 Formation = Berea sandstone (from Rosenbaum, 1974)

K_s (Pa)	ρ_s (kg m^{-3})	α_m (ms^{-1})	β_m (ms^{-1})	$\tilde{\phi}$ %
3.79 10^{10}	2650	3670	2170	19

1.2 Saturant fluids.

	α_f (ms^{-1})	ρ_f (kg m^{-3})	η (cp)
Oil[1]	1455.4	879.4	180
Water	1500	1000	1
Gaseous water 1[2]	800	1000	1
Gaseous water 2[2]	727.5	941	0.211
Gas[3]	629.7	139.8	0.022

[1] From Kuster and Toksöz (1974b)
[2] see text
[3] From Rosenbaum (1974)

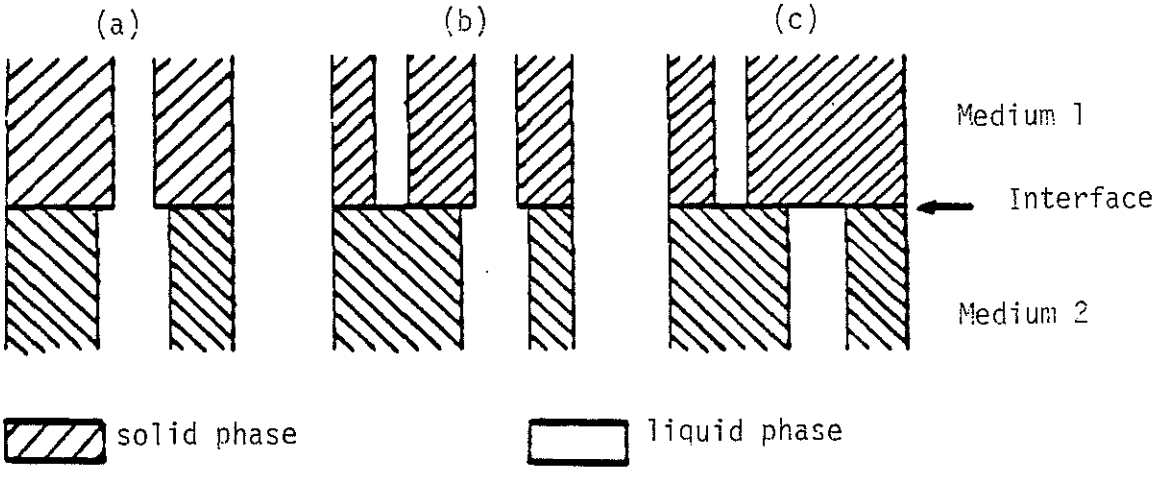

Figure 1: Simplified diagrams of an interface between two saturated porous media (after Deresiewick and Skalak, 1963).

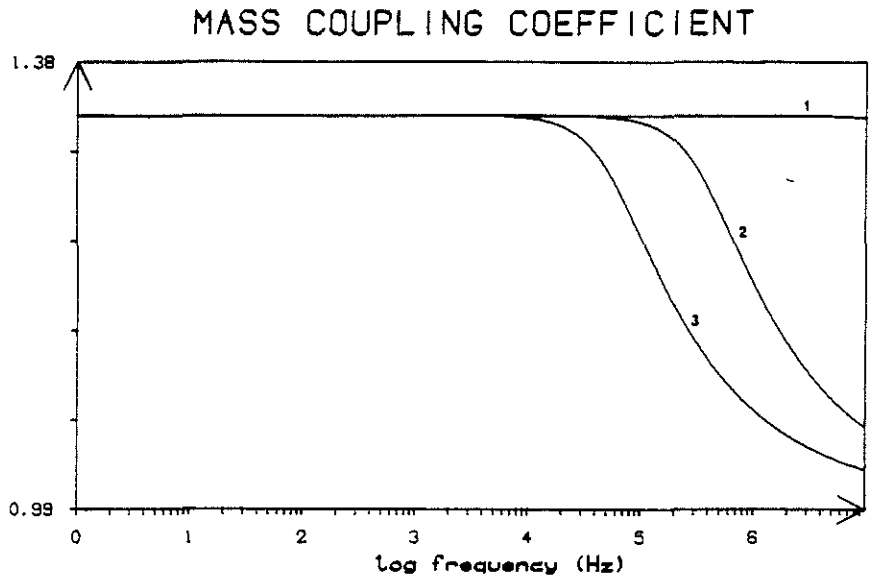

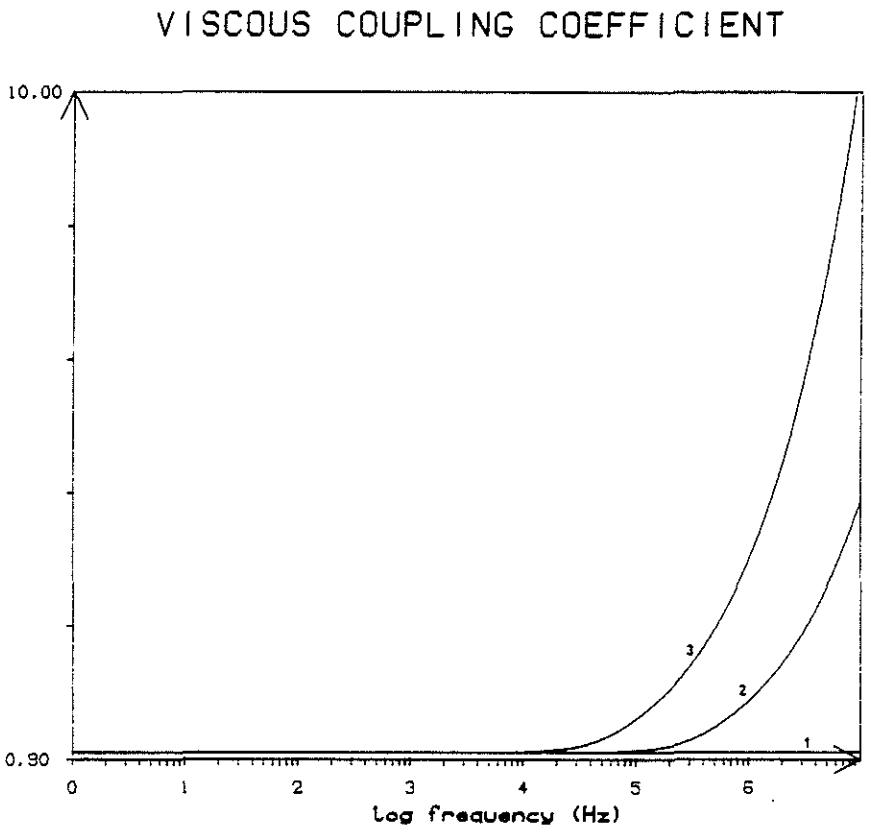

Figure 2a: Berea sandstone. $\tilde{\phi} = 19\%$, $\tilde{k} = 200$md. Saturant fluid effects. 1 = Oil, 2 = Water, 3 = Gas.
Normalized coupling coefficients $(\rho_{22}(\omega)/(\tilde{\phi}\rho_f);\ b(\omega)/(\eta\tilde{\phi}^2/\tilde{k}))$

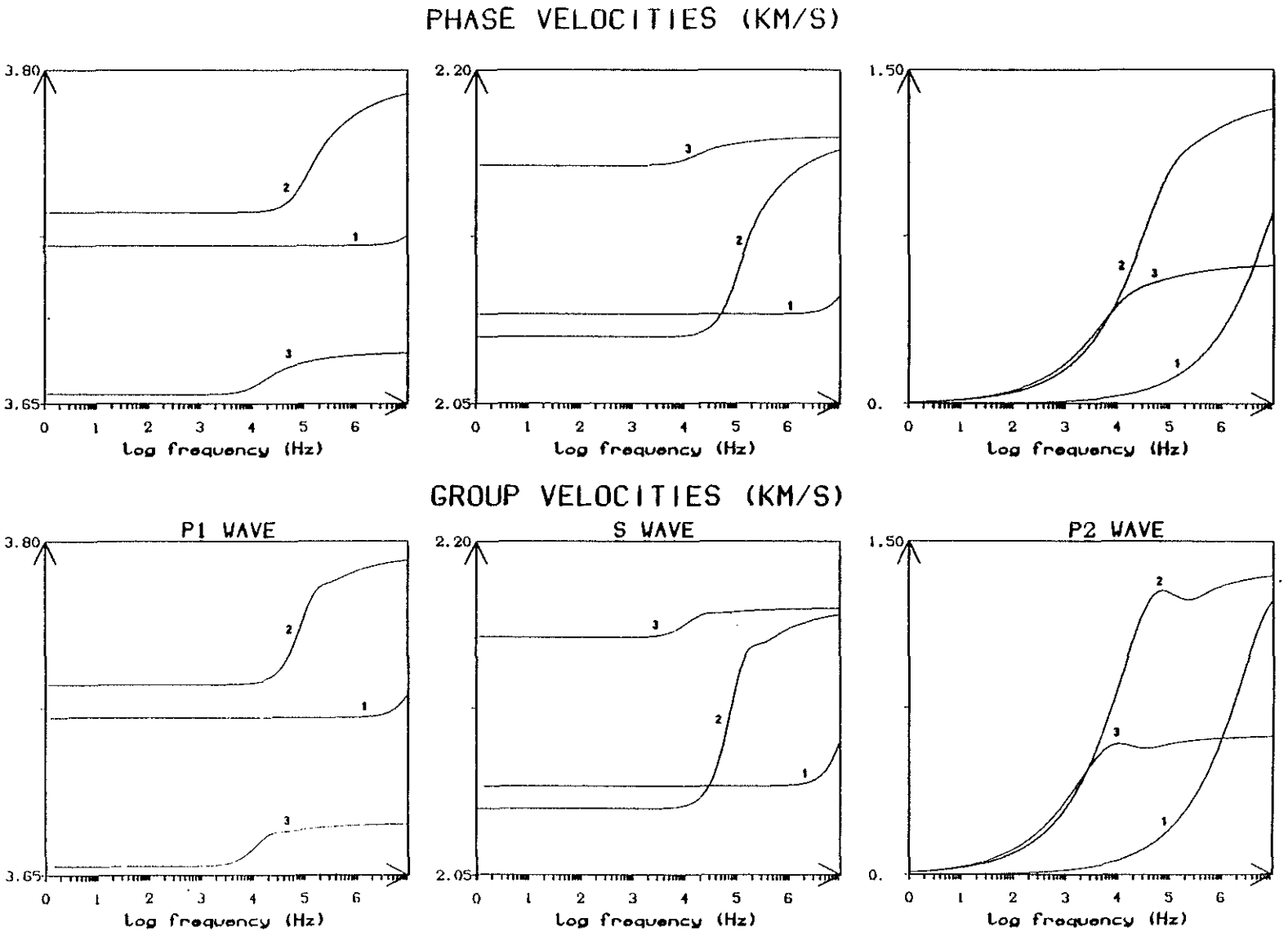

Figure 2b: Berea sandstone. $\tilde{\phi} = 19\%$, $\tilde{k} = 200$md. Saturant fluid effects. 1 = Oil, 2 = Water, 3 = Gas.
Phase and group velocities of the body waves (P_1, S, P_2)

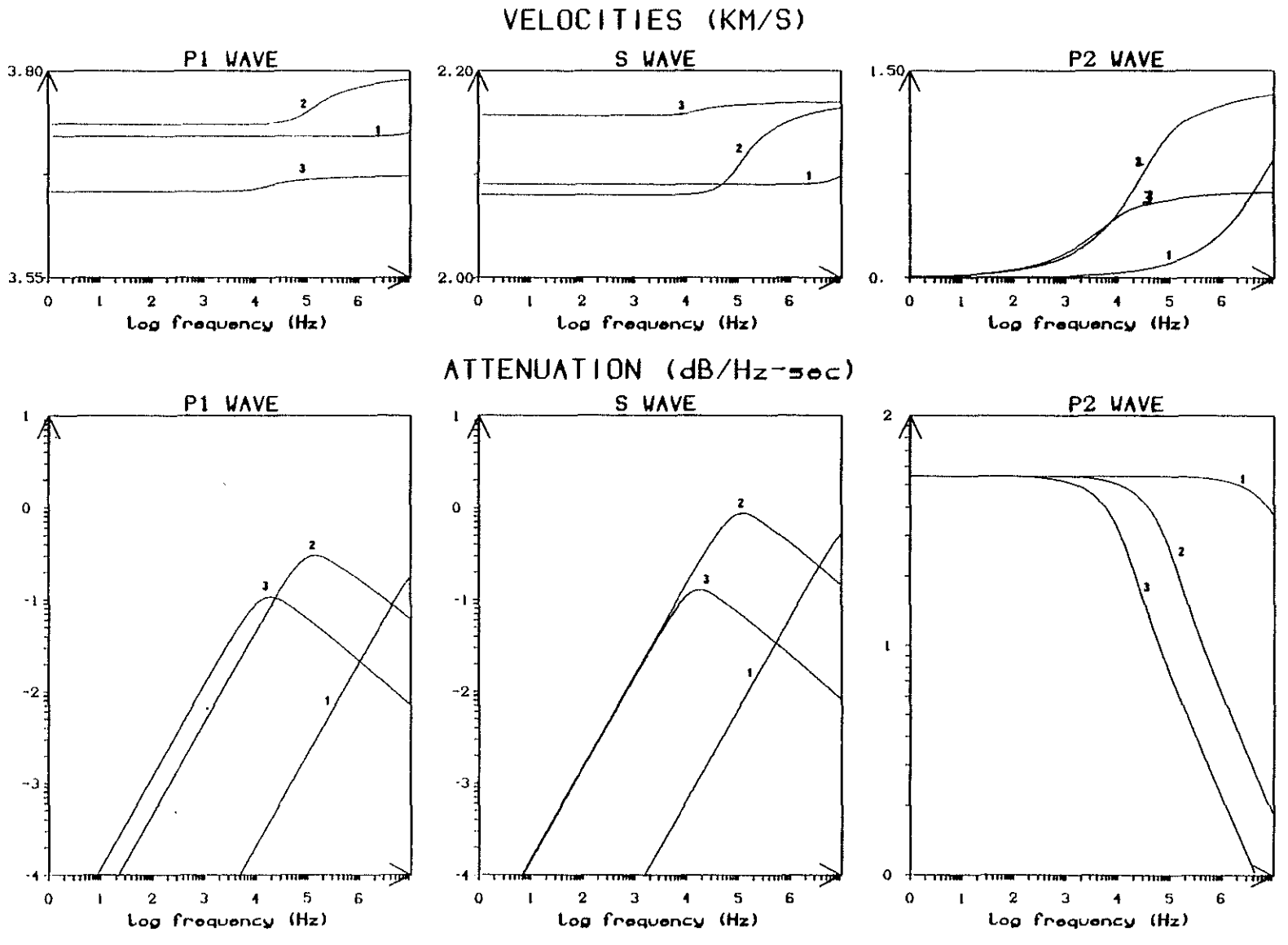

Figure 2c: Berea sandstone. $\tilde{\phi} = 19\%$, $\tilde{k} = 200$md. Saturant fluid effects. 1 = Oil, 2 = Water, 3 = Gas.
Phase velocities and attenuations (dB/ λ) of the body waves

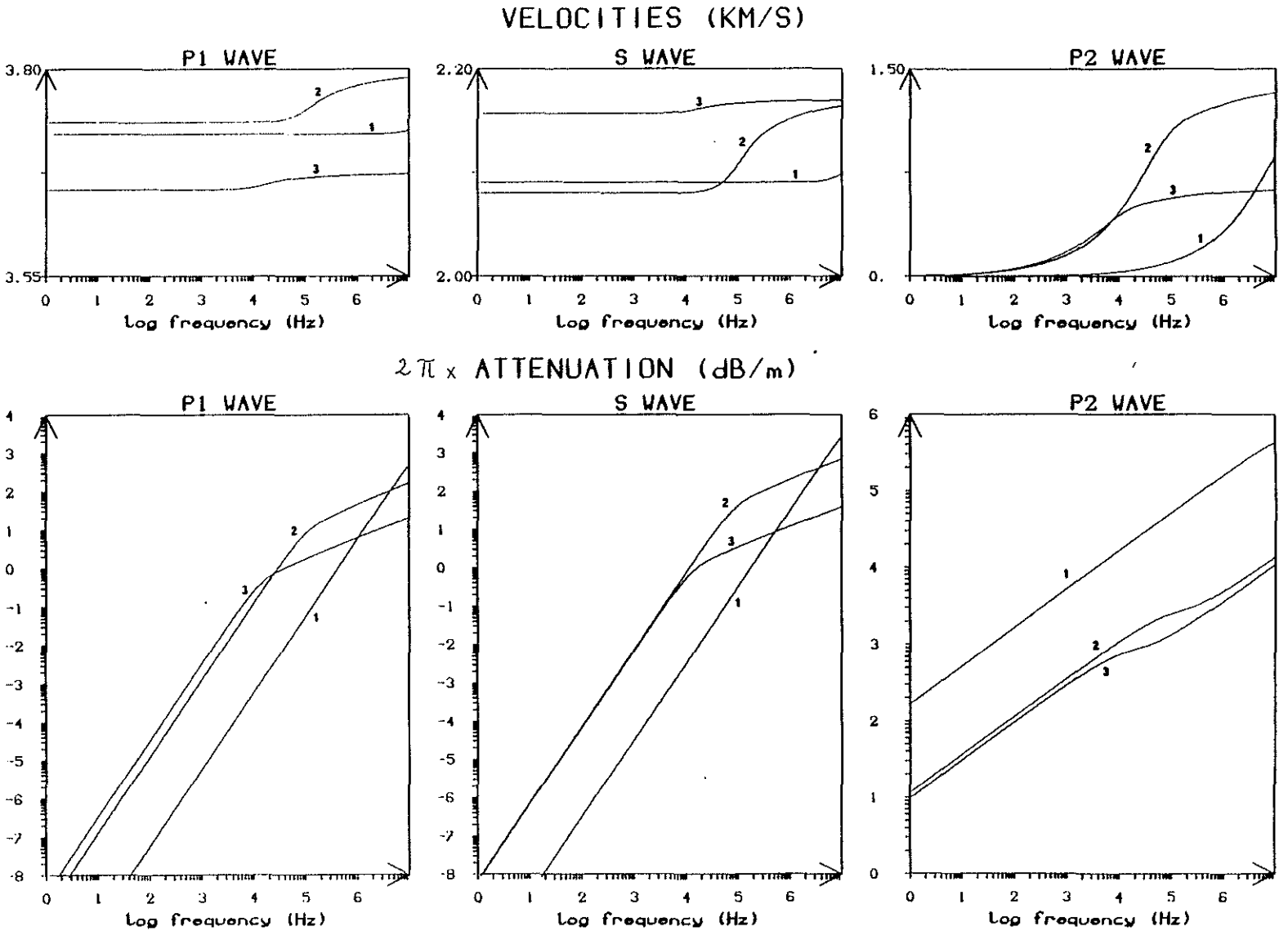

Figure 2d: Berea sandstone. $\tilde{\phi} = 19\%$, $\tilde{k} = 200$md. Saturant fluid effects. 1 = Oil, 2 = Water, 3 = Gas.
Phase velocities and attenuations (dB/m) of the body waves

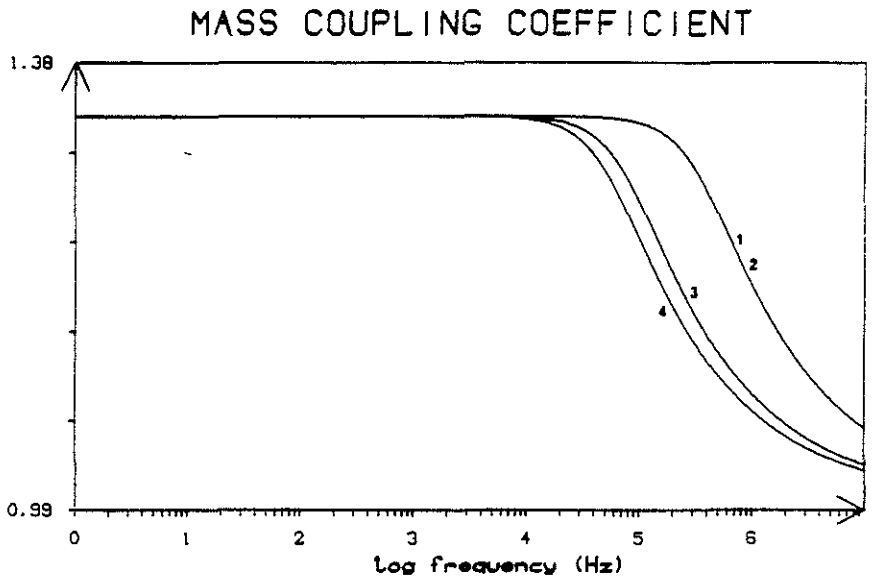

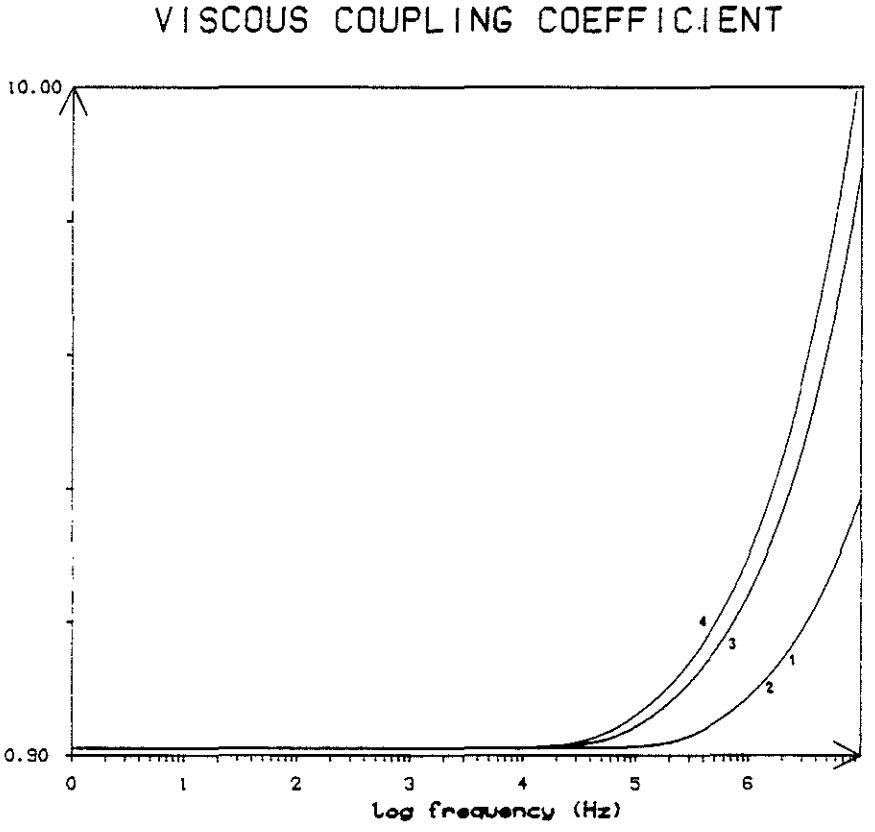

Figure 3a: Berea sandstone $\tilde{\phi} = 19$ %, $\tilde{k} = 200$ md. Saturant fluid effects. 1 = Water, 2 = Gaseous water 1, 3 = Gaseous water 2, 4 = Gas.
Normalized coupling coefficients $(\rho_{22}(\omega)/(\tilde{\phi}\rho_f); b(\omega)/(\eta\tilde{\phi}^2/\tilde{k}))$

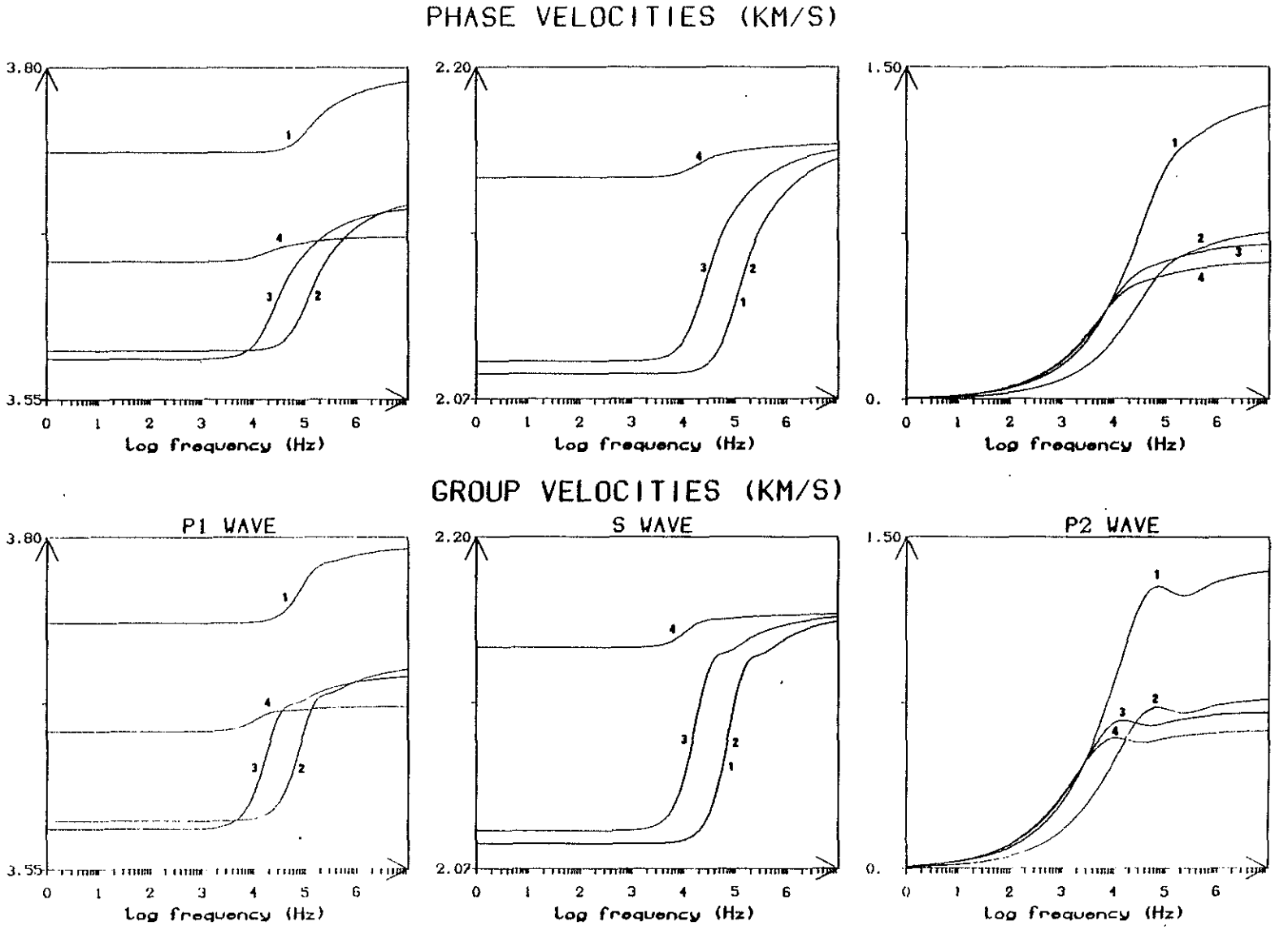

Figure 3b: Berea sandstone $\tilde{\phi} = 19$ %, $\tilde{k} = 200$ md. Saturant fluid effects. 1 = Water, 2 = Gaseous water 1, 3 = Gaseous water 2, 4 = Gas.
Phase and group velocities of the body waves (P_1, S, P_2)

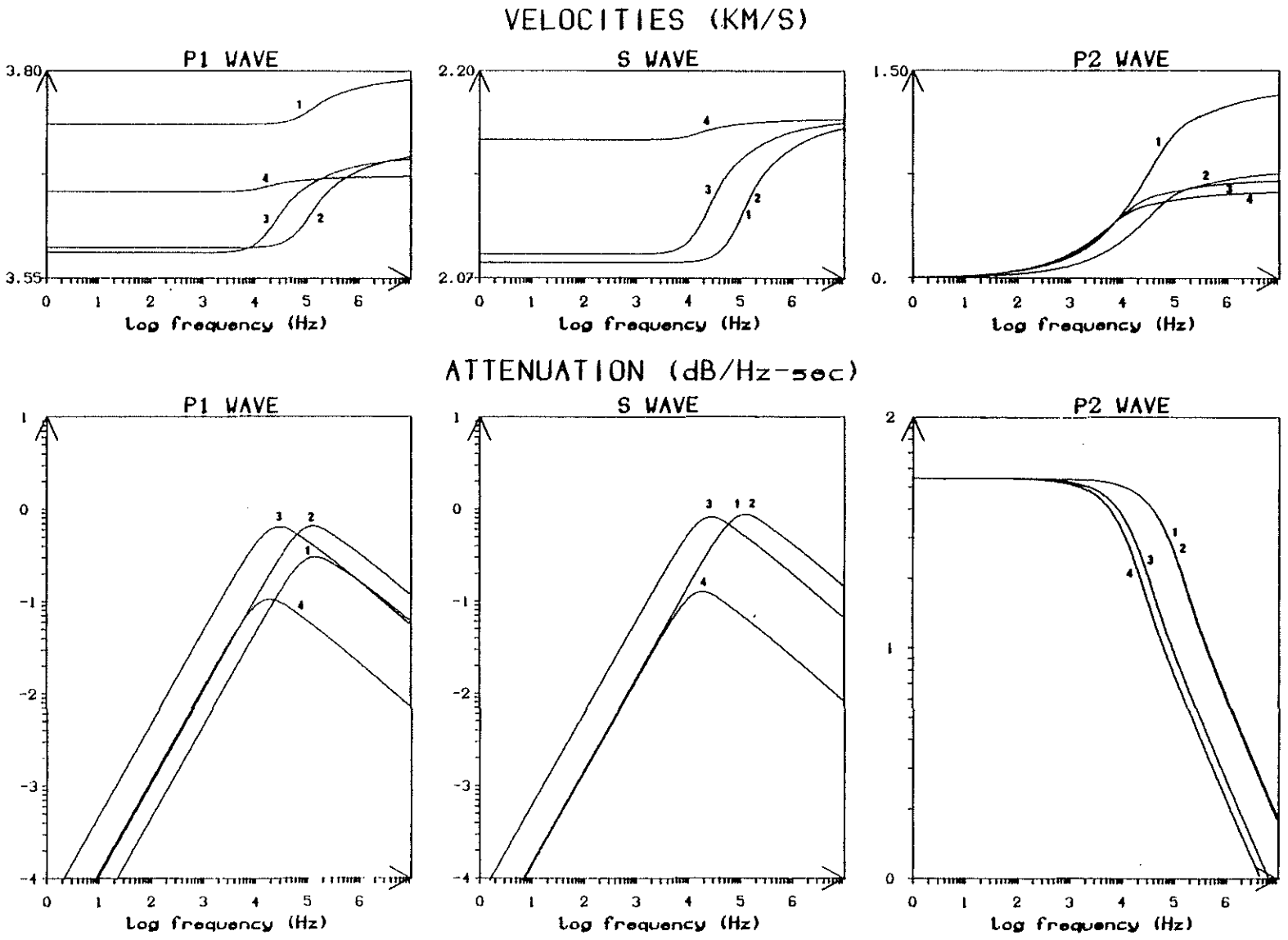

Figure 3c: Berea sandstone $\tilde{\phi} = 19$ %, $\tilde{k} = 200$ md. Saturant fluid effects. 1 = Water, 2 = Gaseous water 1, 3 = Gaseous water 2, 4 = Gas.
Phase velocities and attenuations (dB/ λ) of the body waves

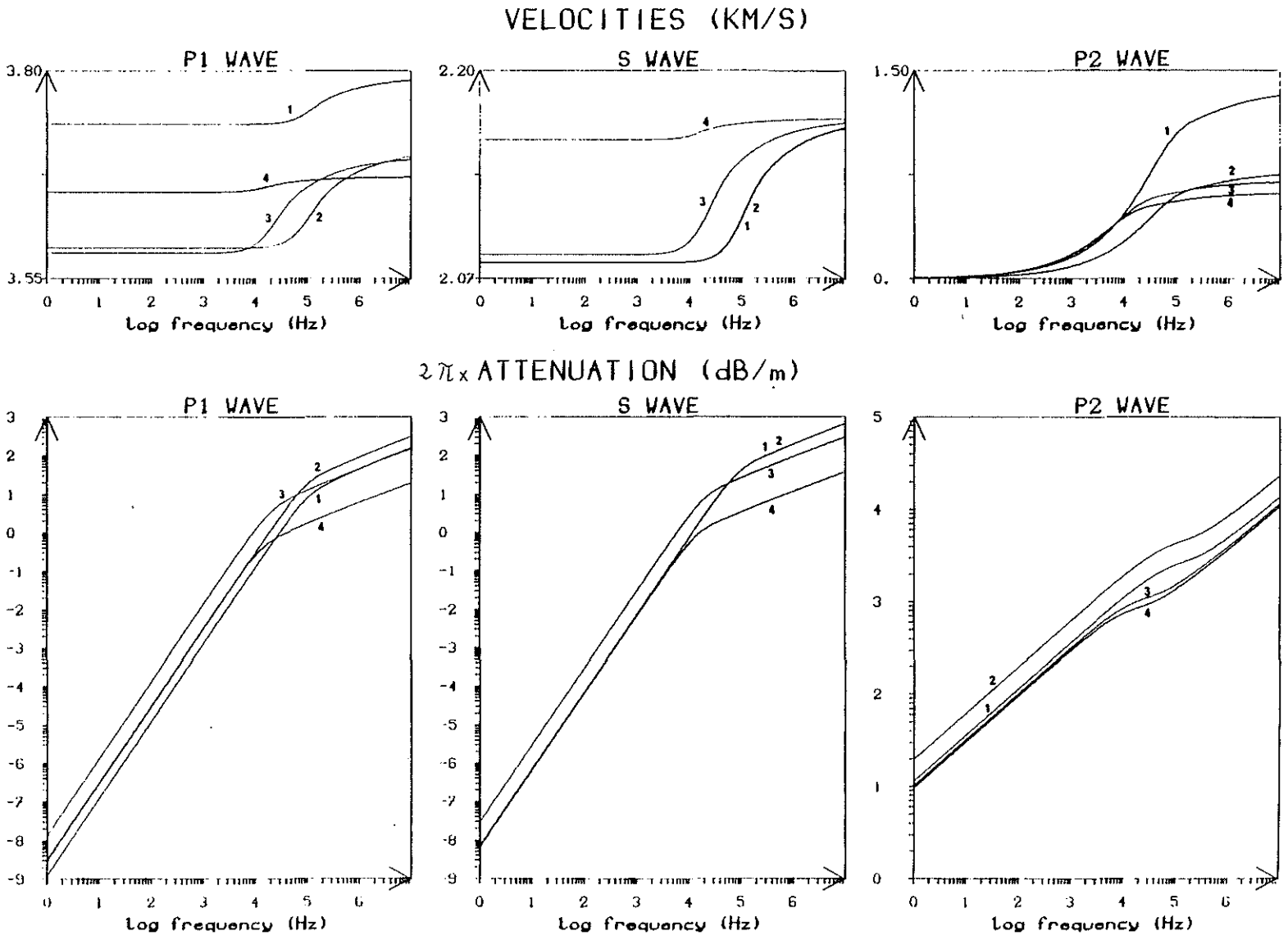

Figure 3d: Berea sandstone $\tilde{\phi} = 19$ %, $\tilde{k} = 200$ md. Saturant fluid effects. 1 = Water, 2 = Gaseous water 1, 3 = Gaseous water 2, 4 = Gas.
Phase velocities and attenuations (dB/m) of the body waves

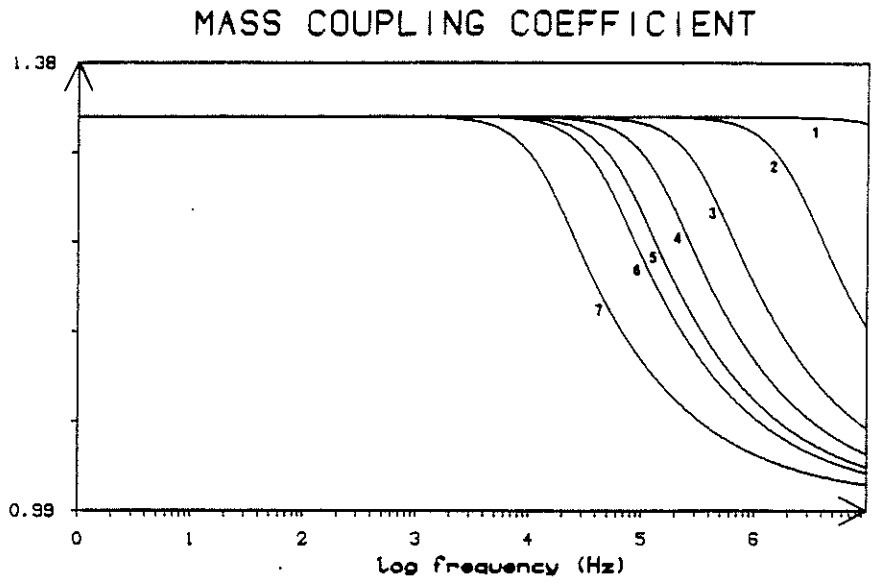

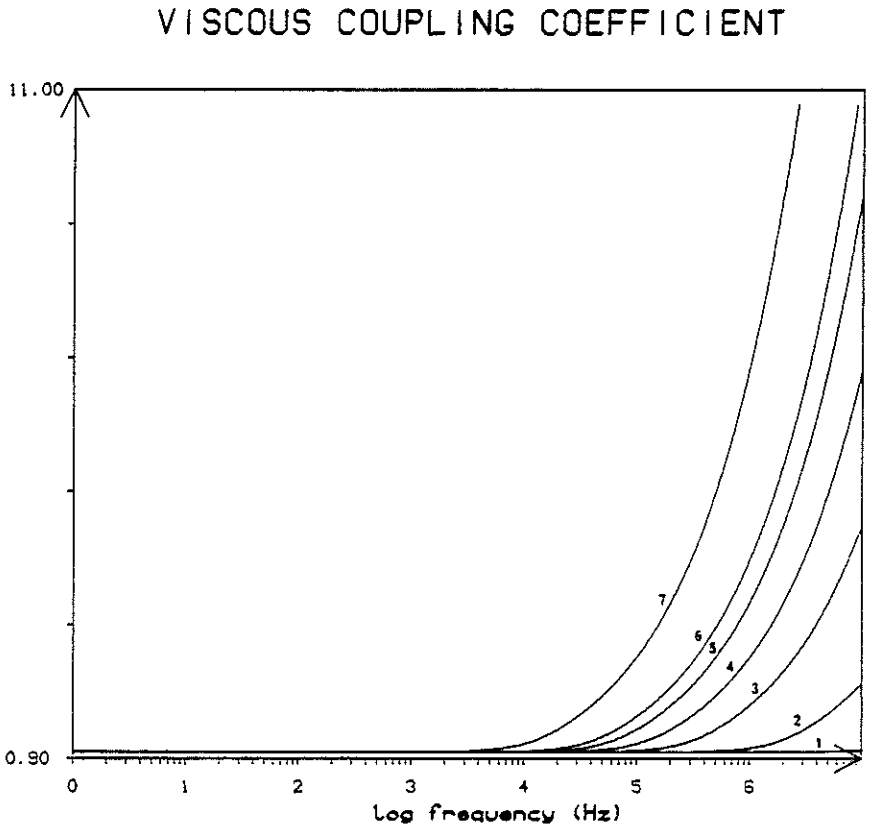

Figure 4a: Berea sandstone. $\tilde{\phi} = 19\%$. Water saturation. Permeability effects. 1: $\tilde{k} =$ 2 md, 2: $\tilde{k} = 32.5$ md, 3: $\tilde{k} = 200$ md, 4: $\tilde{k} = 500$ md, 5: $\tilde{k} = 1$ darcy, 6: $\tilde{k} = 1.5$ darcy, 7: $\tilde{k} = 5$ d.
Normalized coupling coefficients $(\rho_{22}(\omega)/(\tilde{\phi}\rho_f)$; $b(\omega)/(\eta\tilde{\phi}^2/\tilde{k}))$

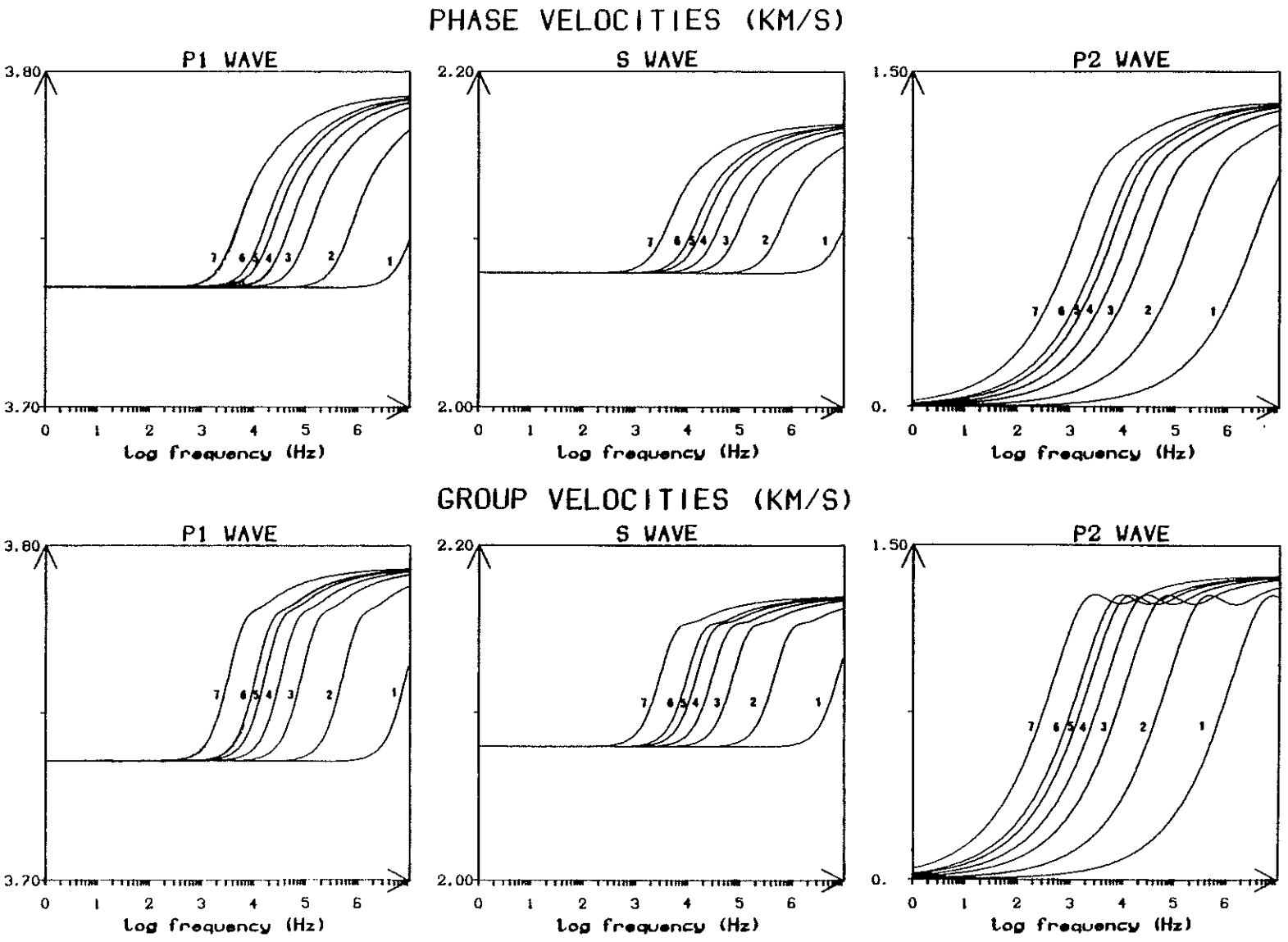

Figure 4b: Berea sandstone. $\tilde{\phi} = 19\%$. Water saturation. Permeability effects. 1: $\tilde{k} =$ 2 md, 2: $\tilde{k} = 32.5$ md, 3: $\tilde{k} = 200$ md, 4: $\tilde{k} = 500$ md, 5: $\tilde{k} = 1$ darcy, 6: $\tilde{k} = 1.5$ darcy, 7: $\tilde{k} = 5$ d.
Phase and group velocities of the body waves (P_1, S, P_2)

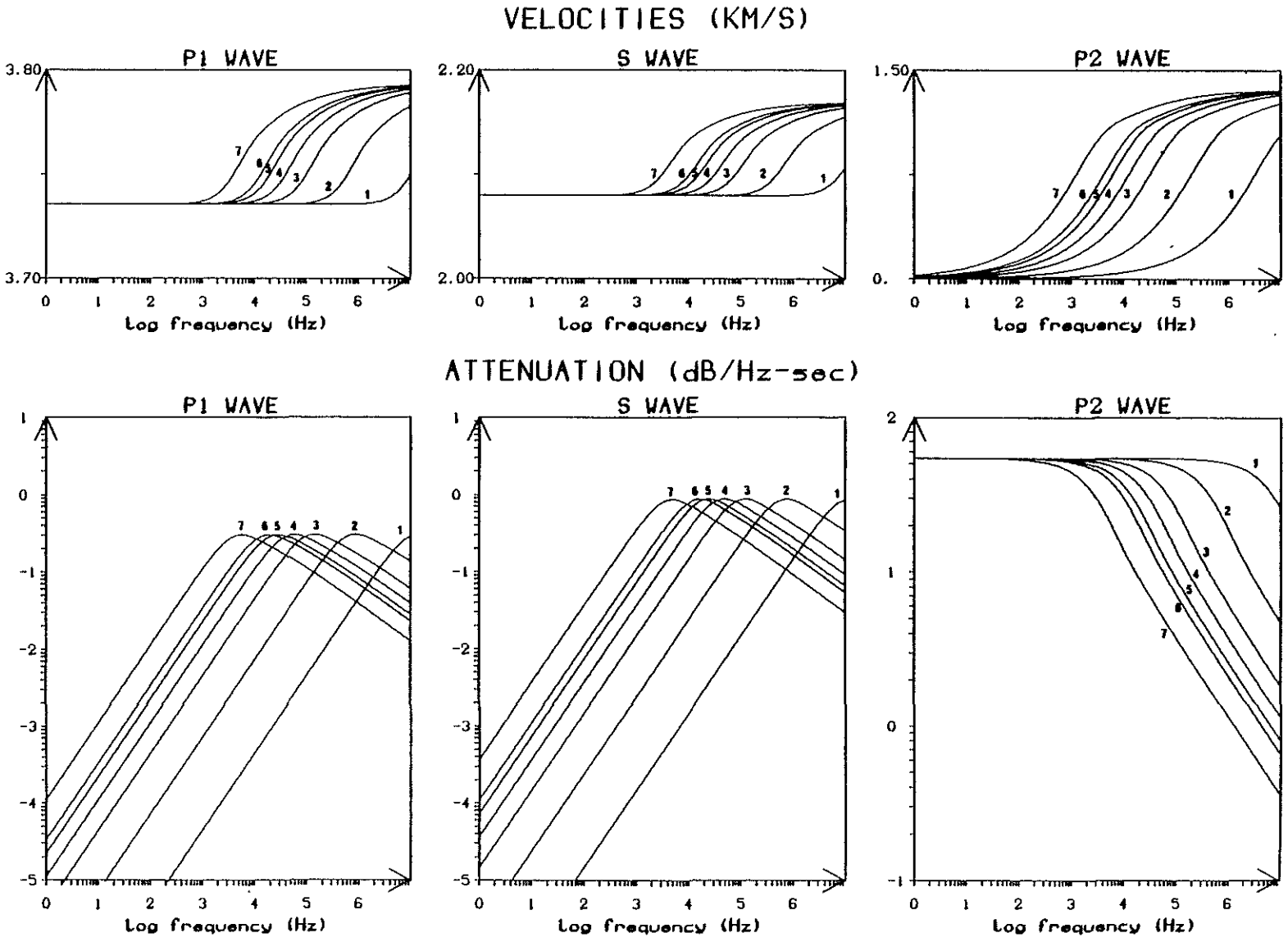

Figure 4c: Berea sandstone. $\tilde{\phi} = 19\%$. Water saturation. Permeability effects. 1: $\tilde{k} =$ 2 md, 2: $\tilde{k} = 32.5$ md, 3: $\tilde{k} = 200$ md, 4: $\tilde{k} = 500$ md, 5: $\tilde{k} = 1$ darcy, 6: $\tilde{k} = 1.5$ darcy, 7: $\tilde{k} = 5$ d.
Phase velocities and attenuations (dB/ λ) of the body waves

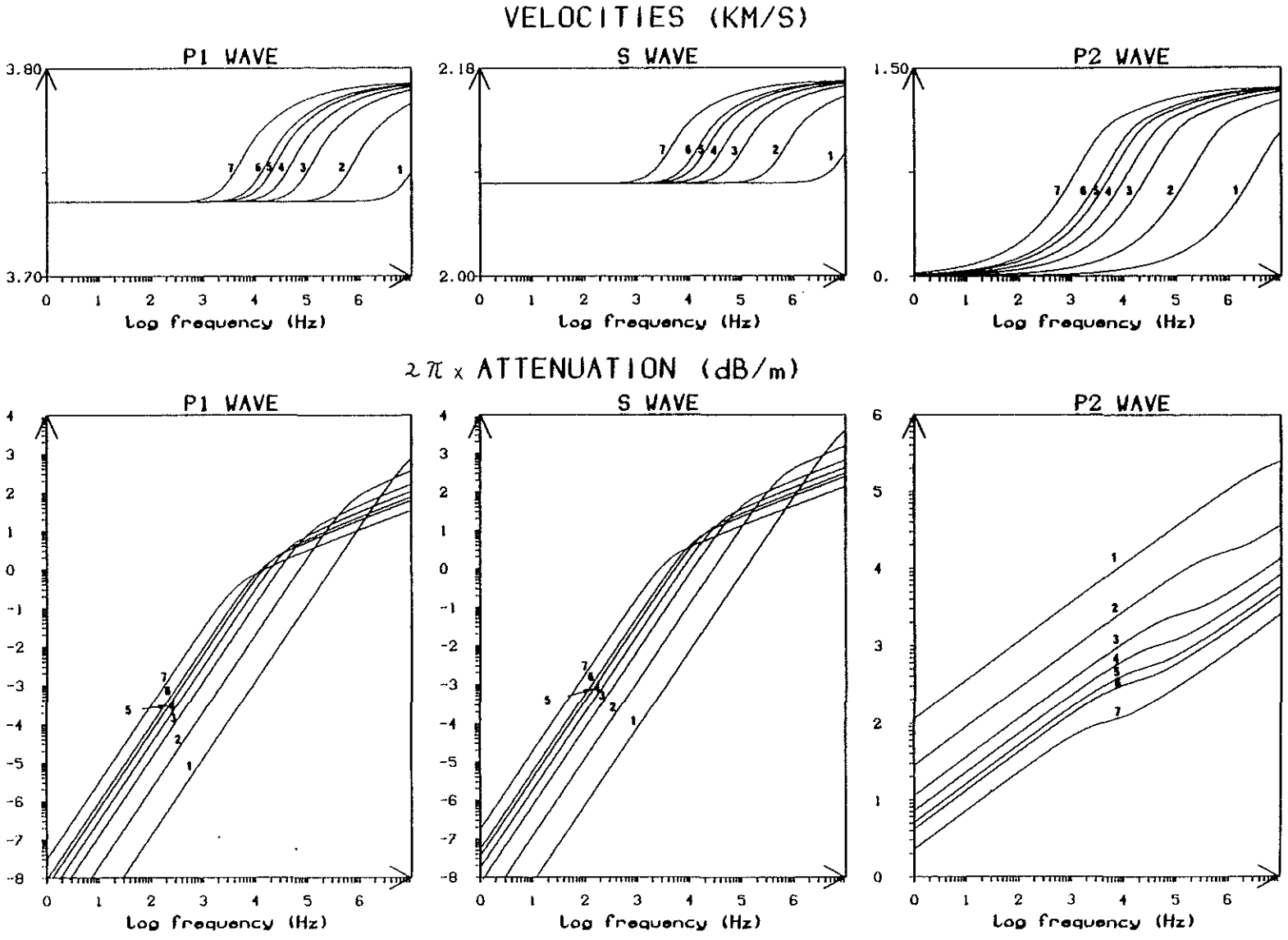

Figure 4d: Berea sandstone. $\tilde{\phi} = 19\%$. Water saturation. Permeability effects. 1: $\tilde{k} =$ 2 md, 2: $\tilde{k} = 32.5$ md, 3: $\tilde{k} = 200$ md, 4: $\tilde{k} = 500$ md, 5: $\tilde{k} = 1$ darcy, 6: $\tilde{k} = 1.5$ darcy, 7: $\tilde{k} = 5$ d.
Phase velocities and attenuations (dB/m) of the body waves

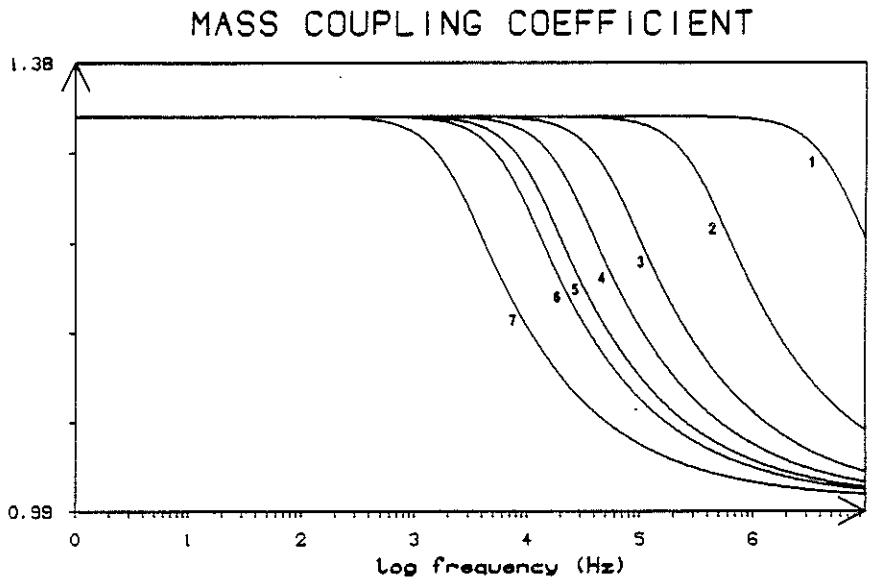

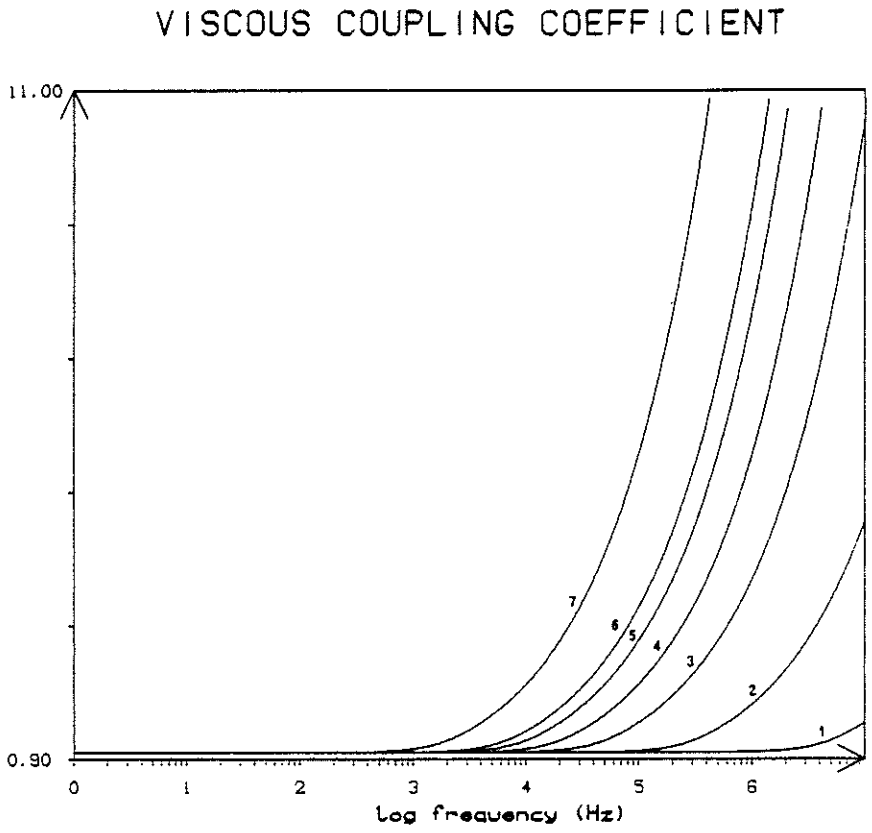

Figure 5a: Berea sandstone. $\tilde{\phi} = 19\%$. Gas saturation. Permeability effects. 1: $\tilde{k} = 2$ md, 2: $\tilde{k} = 32.5$ md, 3: $\tilde{k} = 200$ md, 4: $\tilde{k} = 500$ md, 5: $\tilde{k} = 1$ darcy, 6: $\tilde{k} = 1.5$ darcy, 7: $\tilde{k} = 5$ d.
Normalized coupling coefficients $(\rho_{22}(\omega)/(\tilde{\phi}\rho_f);\ b(\omega)/(\eta\tilde{\phi}^2/\tilde{k}))$

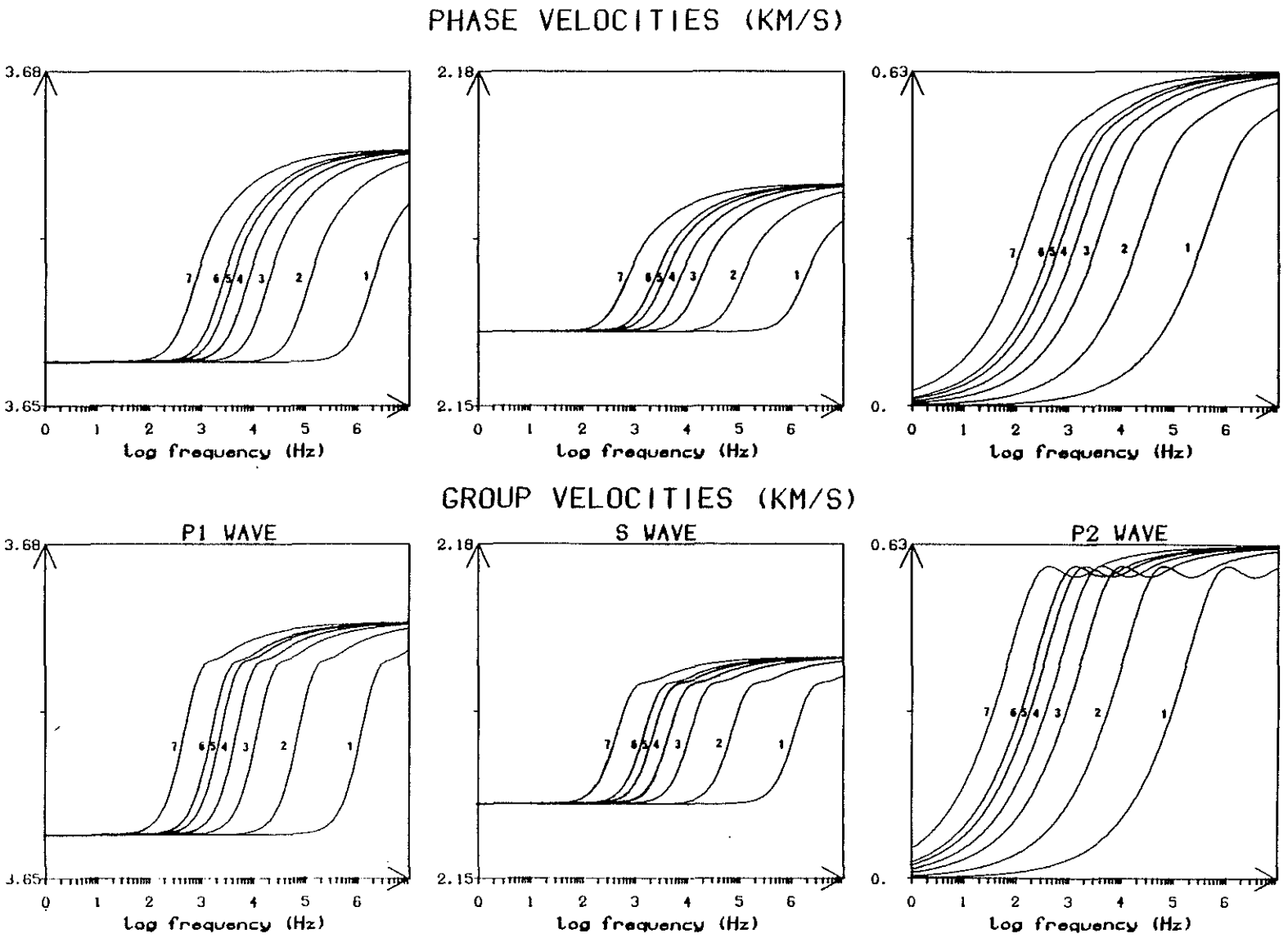

Figure 5b: Berea sandstone. $\tilde{\phi} = 19\%$. Gas saturation. Permeability effects. 1: $\tilde{k} = 2$ md, 2: $\tilde{k} = 32.5$ md, 3: $\tilde{k} = 200$ md, 4: $\tilde{k} = 500$ md, 5: $\tilde{k} = 1$ darcy, 6: $\tilde{k} = 1.5$ darcy, 7: $\tilde{k} = 5$ d.
Phase and group velocities of the body waves (P_1, S, P_2)

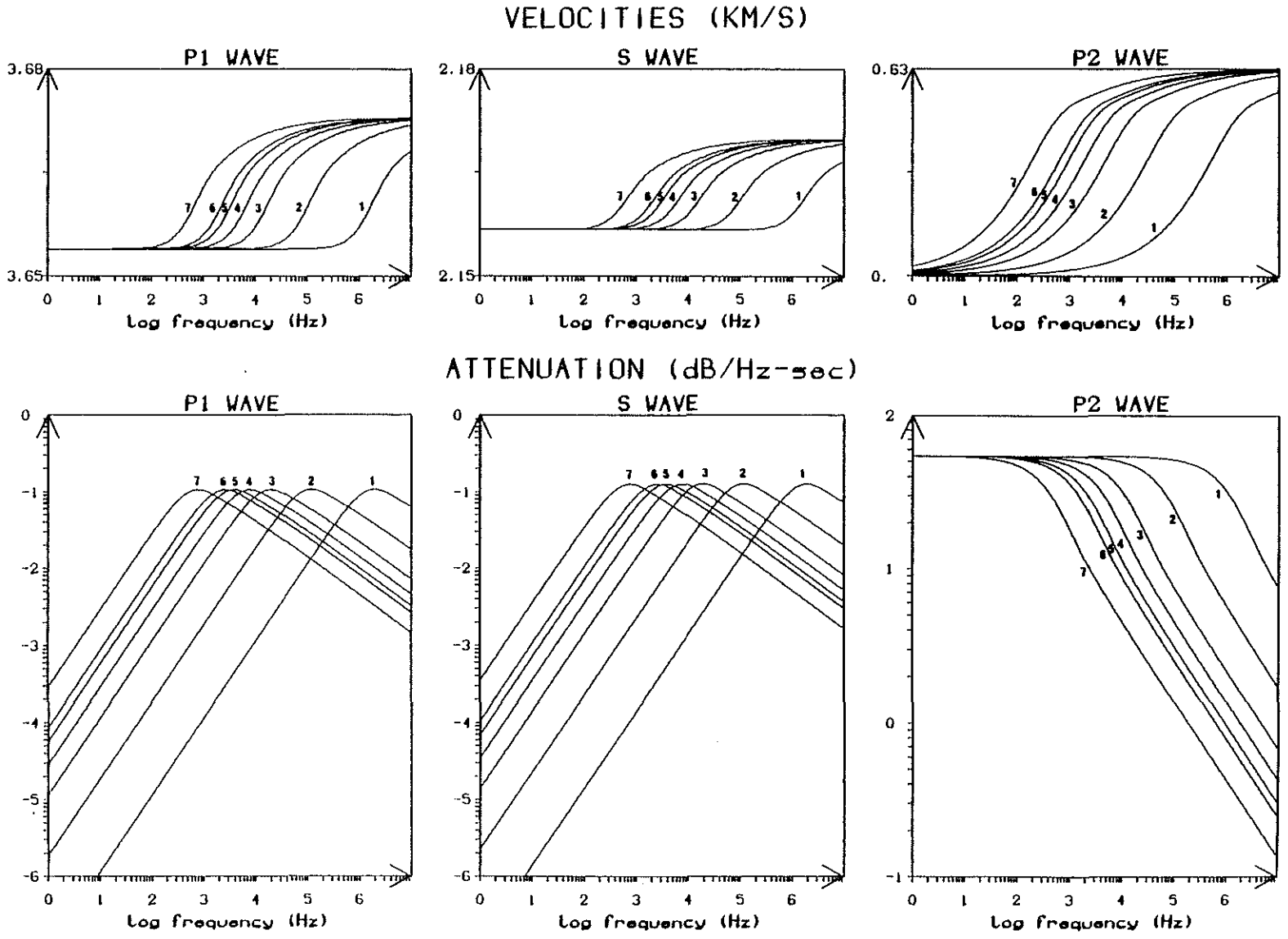

Figure 5c: Berea sandstone. $\tilde{\phi} = 19\%$. Gas saturation. Permeability effects. 1: $\tilde{k} = 2$ md, 2: $\tilde{k} = 32.5$ md, 3: $\tilde{k} = 200$ md, 4: $\tilde{k} = 500$ md, 5: $\tilde{k} = 1$ darcy, 6: $\tilde{k} = 1.5$ darcy, 7: $\tilde{k} = 5$ d.
Phase velocities and attenuations (dB/ λ) of the body waves

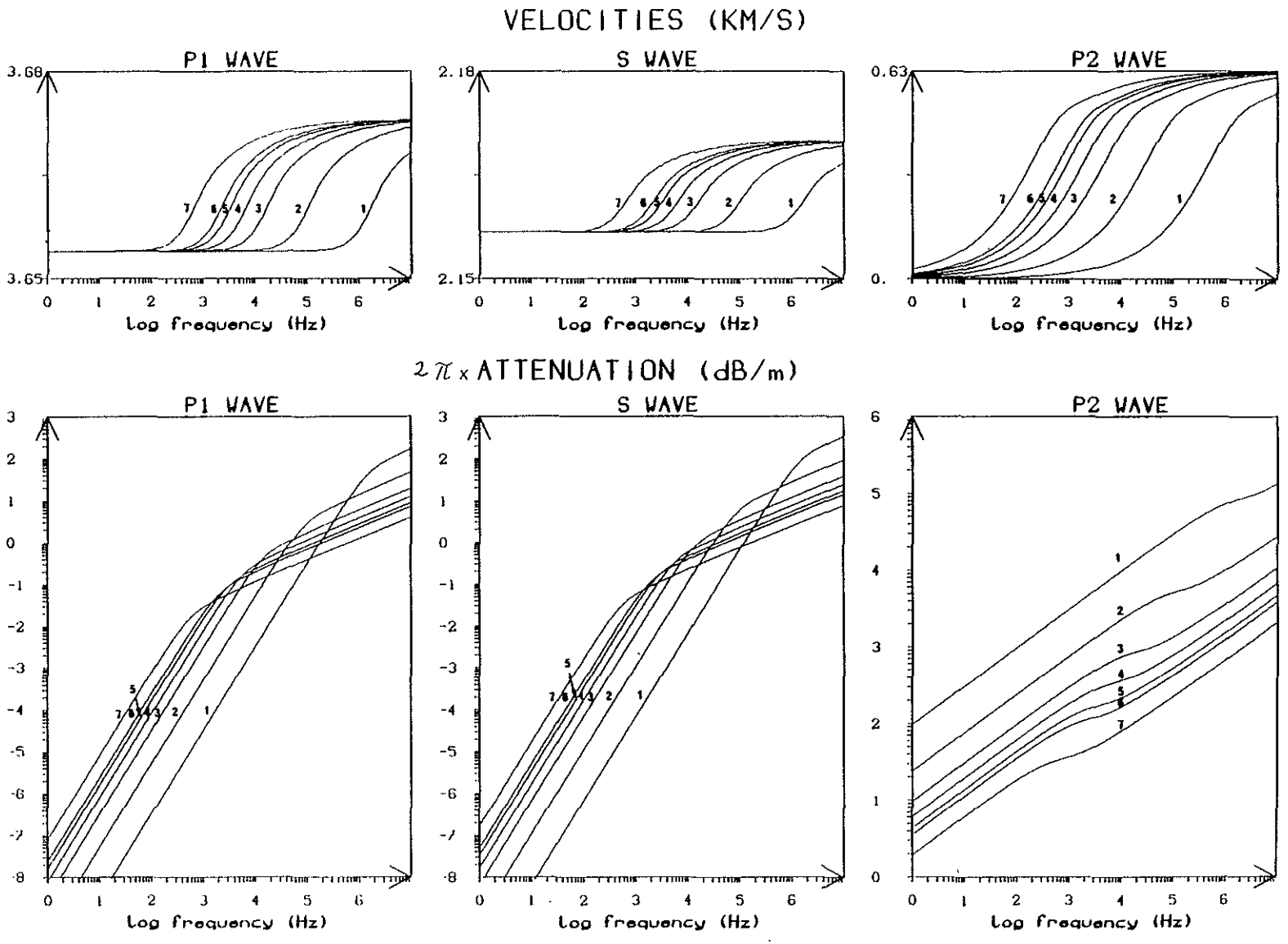

Figure 5d: Berea sandstone. $\tilde{\phi} = 19\%$. Gas saturation. Permeability effects. 1: $\tilde{k} = 2$ md, 2: $\tilde{k} = 32.5$ md, 3: $\tilde{k} = 200$ md, 4: $\tilde{k} = 500$ md, 5: $\tilde{k} = 1$ darcy, 6: $\tilde{k} = 1.5$ darcy, 7: $\tilde{k} = 5$ d.
Phase velocities and attenuations (dB/m) of the body waves

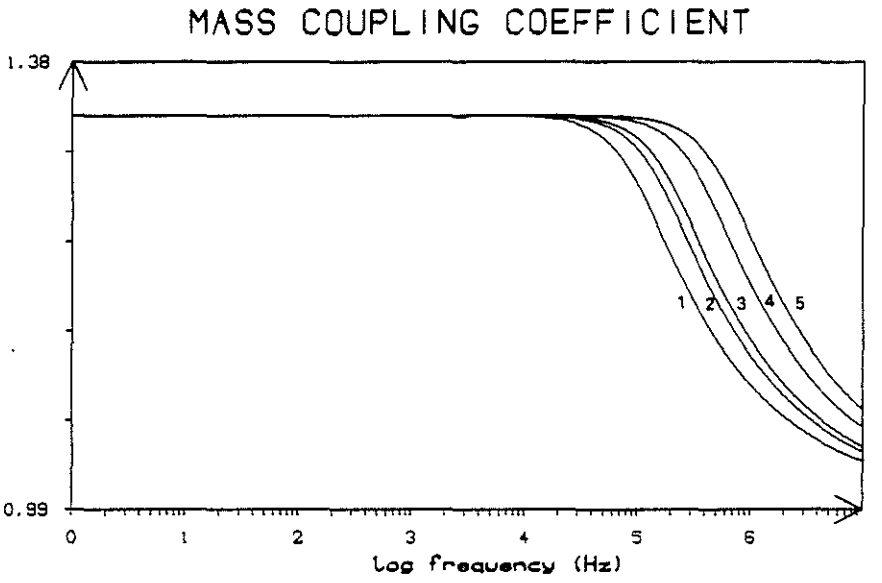

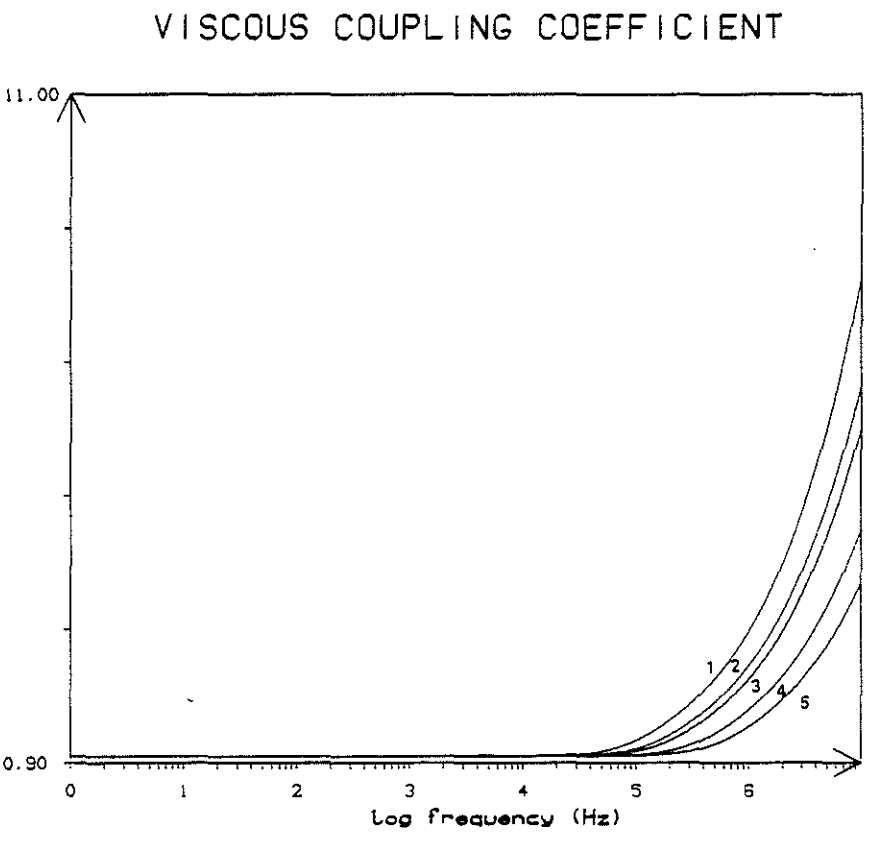

Figure 6a: Berea sandstone. $\tilde{k} = 200$ md. Water saturation. Porosity effects. 1: $\tilde{\phi} = 5\%$, 2: $\tilde{\phi} = 8\%$, 3: $\tilde{\phi} = 10\%$, 4: $\tilde{\phi} = 19\%$, 5: $\tilde{\phi} = 30\%$, Normalized coupling coefficients $(\rho_{22}(\omega)/(\tilde{\phi}\rho_f); b(\omega)/(\eta\tilde{\phi}^2/\tilde{k}))$

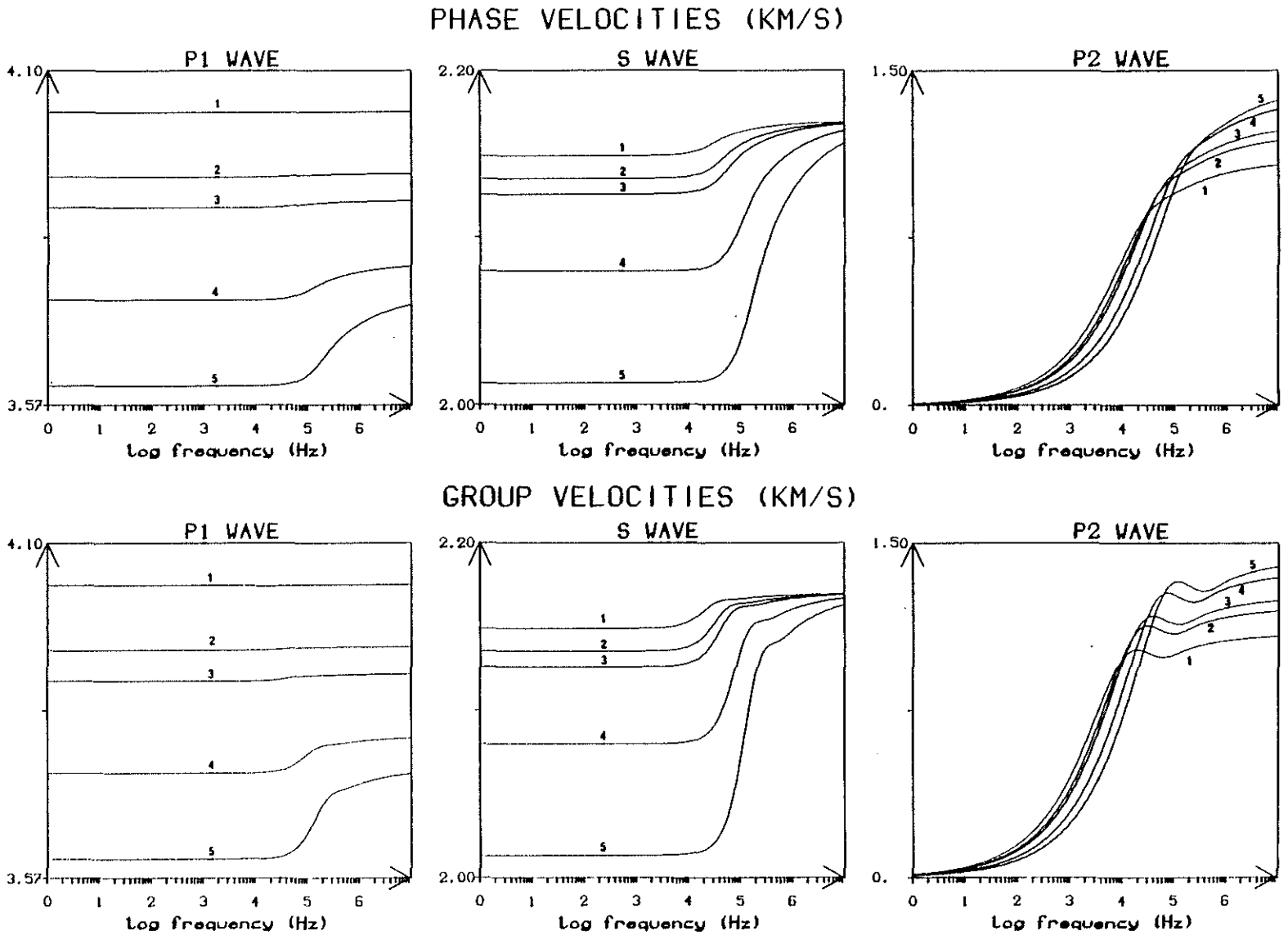

Figure 6b: Berea sandstone. $\tilde{k} = 200$ md. Water saturation. Porosity effects. 1: $\tilde{\phi} = 5\%$, 2: $\tilde{\phi} = 8\%$, 3: $\tilde{\phi} = 10\%$, 4: $\tilde{\phi} = 19\%$, 5: $\tilde{\phi} = 30\%$, Phase and group velocities of the body waves (P_1, S, P_2)

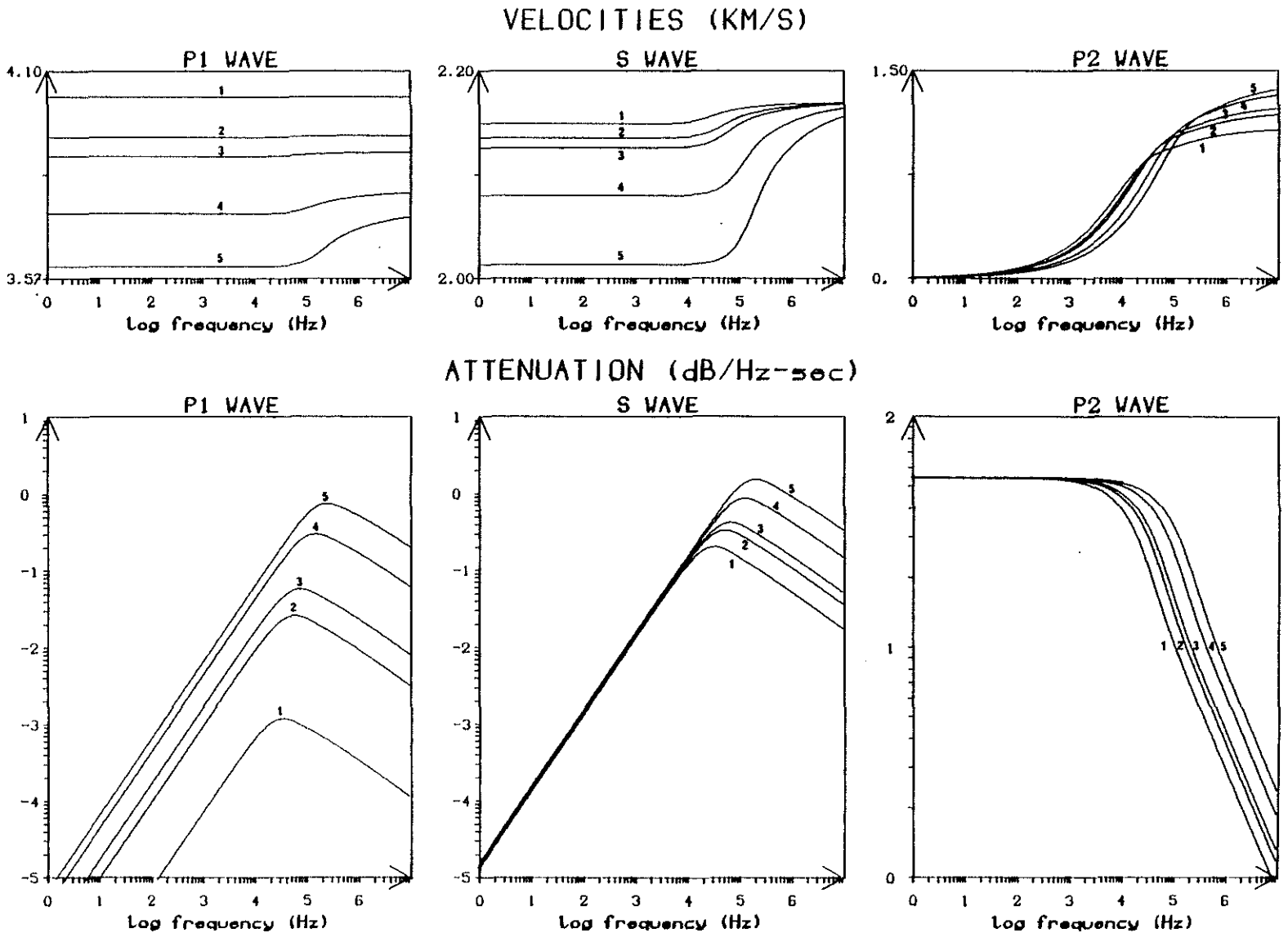

Figure 6c: Berea sandstone. $\tilde{k} = 200$ md. Water saturation. Porosity effects. 1: $\tilde{\phi} = 5\%$, 2: $\tilde{\phi} = 8\%$, 3: $\tilde{\phi} = 10\%$, 4: $\tilde{\phi} = 19\%$, 5: $\tilde{\phi} = 30\%$, Phase velocities and attenuations (dB/ λ) of the body waves

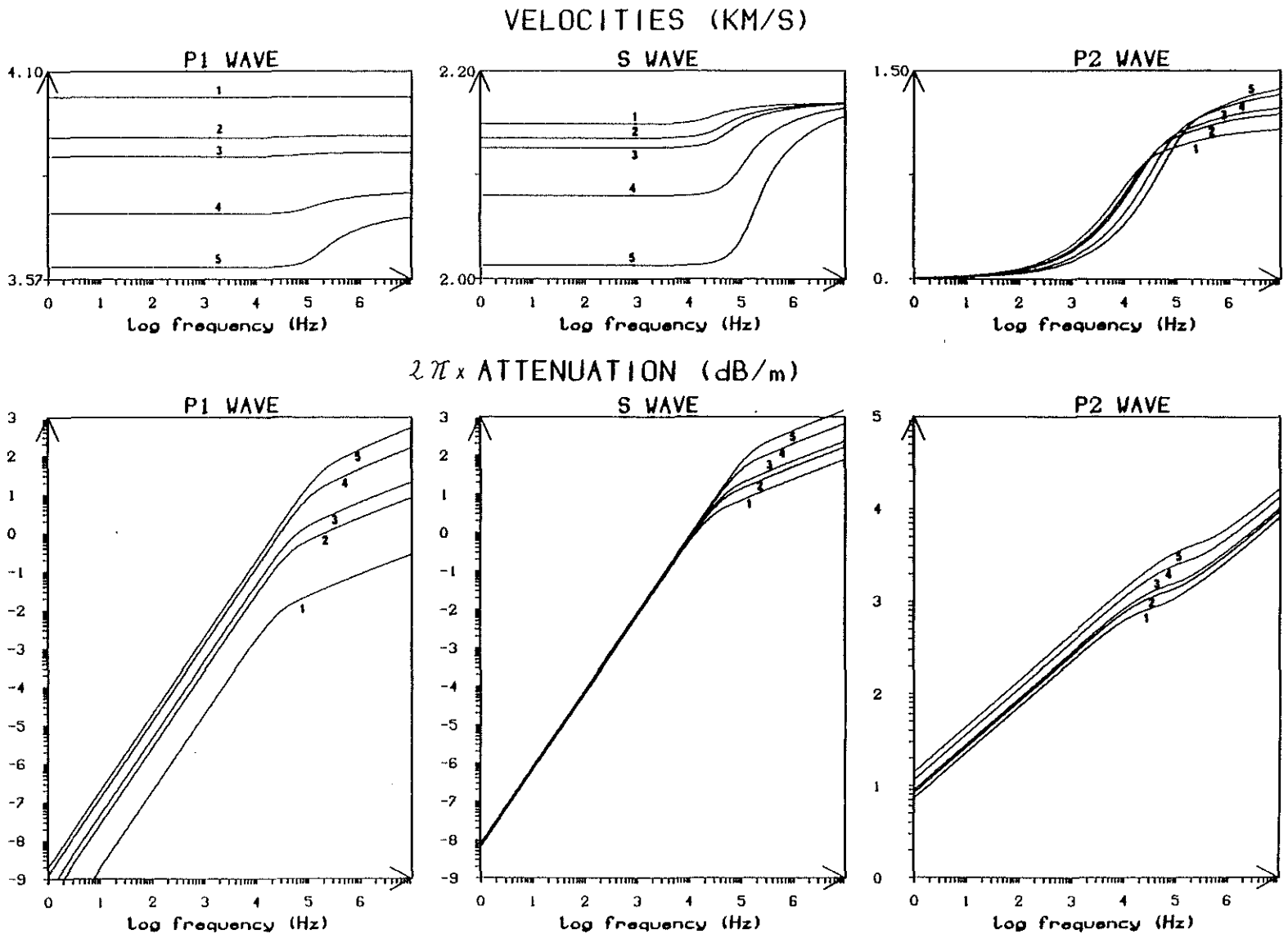

Figure 6d: Berea sandstone. $\tilde{k} = 200$ md. Water saturation. Porosity effects. 1: $\tilde{\phi} = 5\%$, 2: $\tilde{\phi} = 8\%$, 3: $\tilde{\phi} = 10\%$, 4: $\tilde{\phi} = 19\%$, 5: $\tilde{\phi} = 30\%$, Phase velocities and attenuations (dB/m) of the body waves